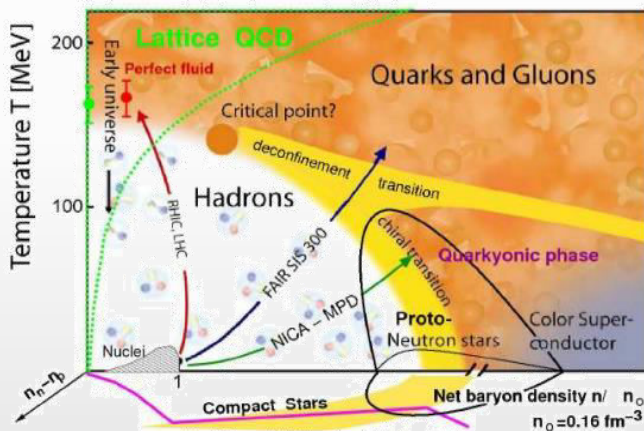
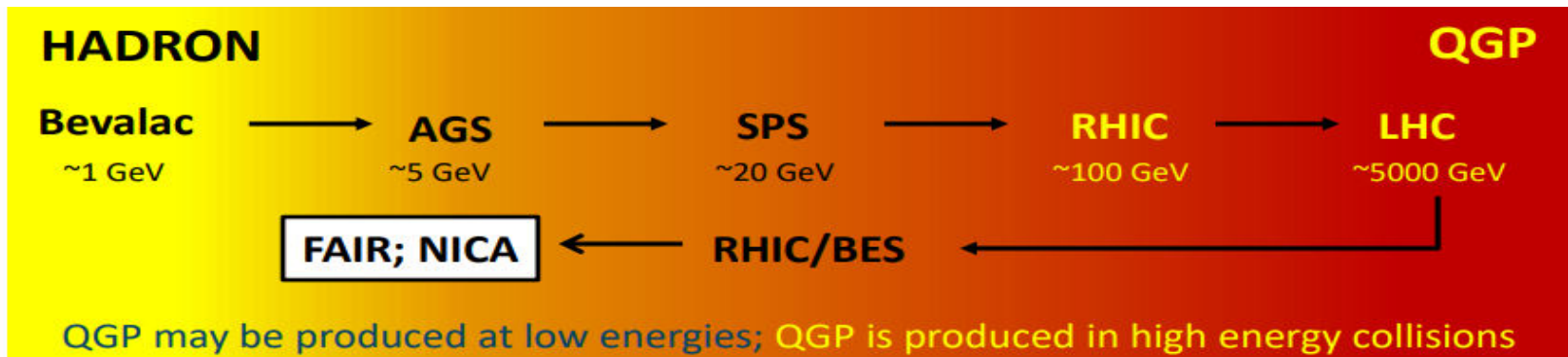


# Status and Physics Program of the MPD-NICA

V. Riabov for the MPD Collaborations

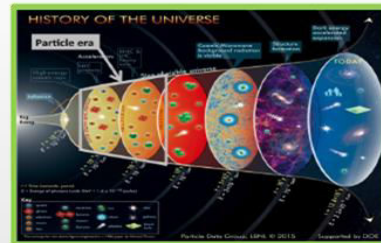


# Heavy-ion collisions



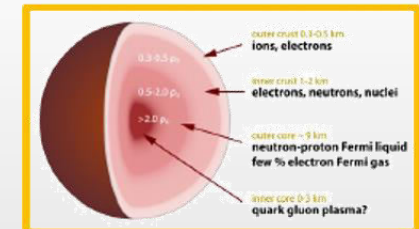
## High beam energies ( $\sqrt{s_{NN}} > 100$ GeV)

High temperature:  
Early Universe evolution



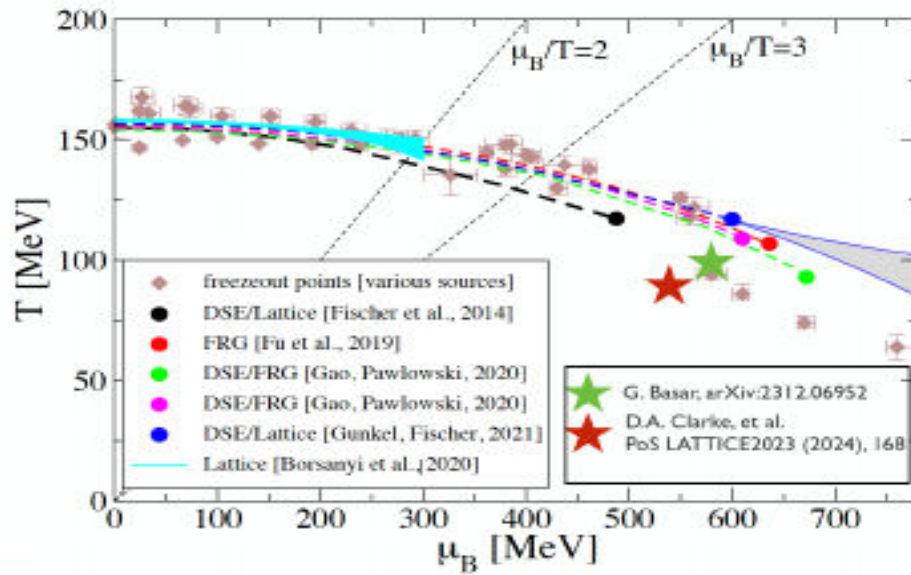
## Low beam energies ( $\sqrt{s_{NN}} \sim 10$ GeV)

high baryon densities  
→ inner structure of  
compact stars



- ❖ At  $\mu_B \sim 0$ , smooth crossover (lattice QCD calculations + data)
- ❖ At large  $\mu_B$ , 1<sup>st</sup> order phase transition → QCD critical point
- ❖ MPD @NICA → study QCD medium at extreme net baryon densities

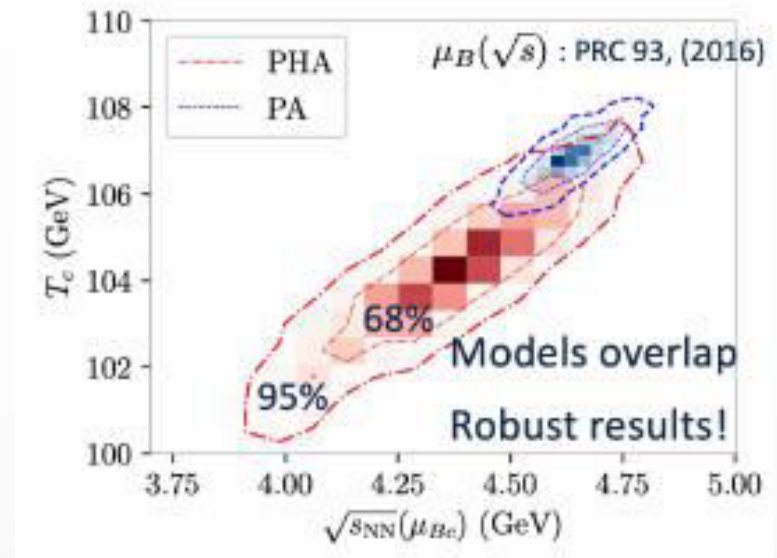
# QCD critical point: predictions/estimations



M. Hippert et al., Phys. Rev. D 110, 094006 (2024)

Method	$\mu_c$ (MeV)	$T_c$ (MeV)
Holography + Bayesian	560 - 625	101 - 108
FRG/DSE	495 - 654	108 - 119
Lee-Yang edge singularities	500 - 600	100 - 105
Lattice QCD	$\mu_c/T_c > 3$	F. Karsch et al.
Summary	495 - 654	100 - 119

$(\mu_c, T_c) = (495 - 654, 100 - 119) \text{ MeV} \rightarrow 3.5 < \sqrt{s_{NN}} < 4.9 \text{ GeV}$

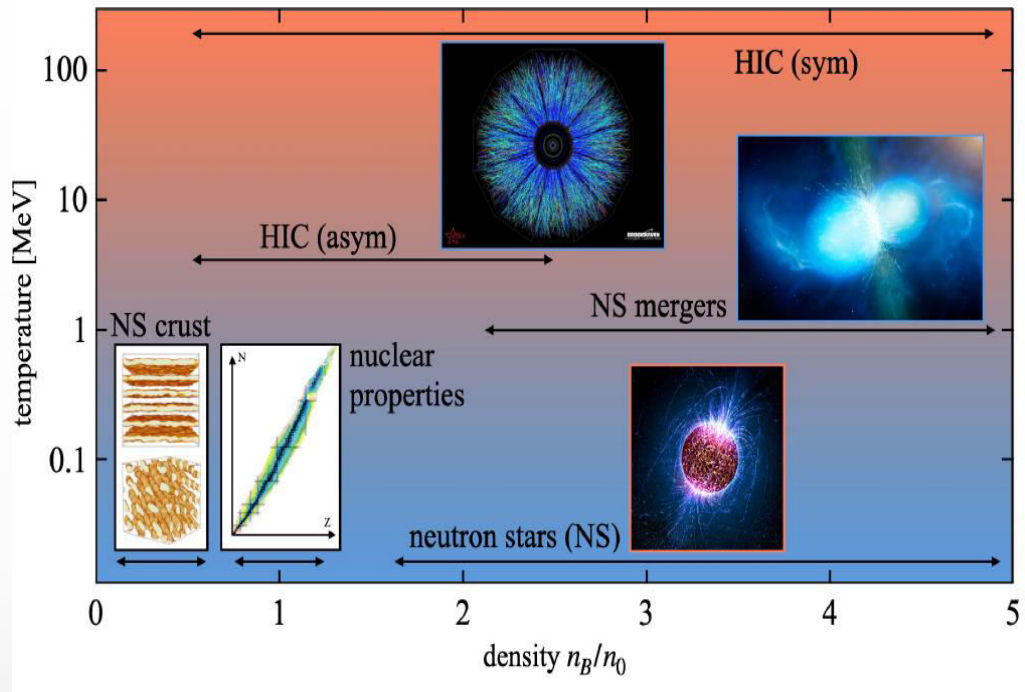


BM@N:  $\sqrt{s_{NN}} = 2.3 - 3.3 \text{ GeV}$   
 MPD:  $\sqrt{s_{NN}} = 2.4 - 11 \text{ GeV}$

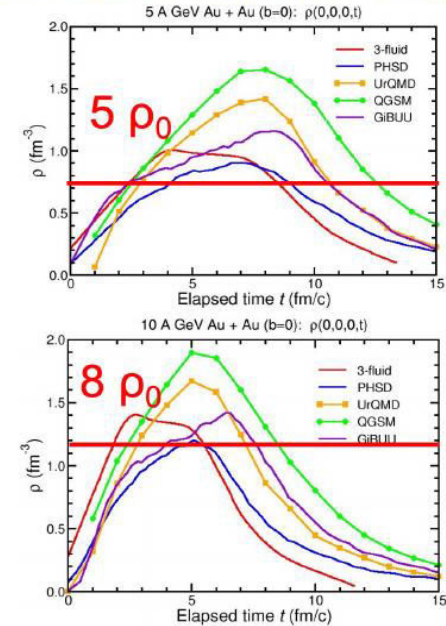
**BM@N and MPD in the collision energy range of the predicted CEP location**



# Dense Nuclear Matter



Baryon densities in central Au+Au collisions



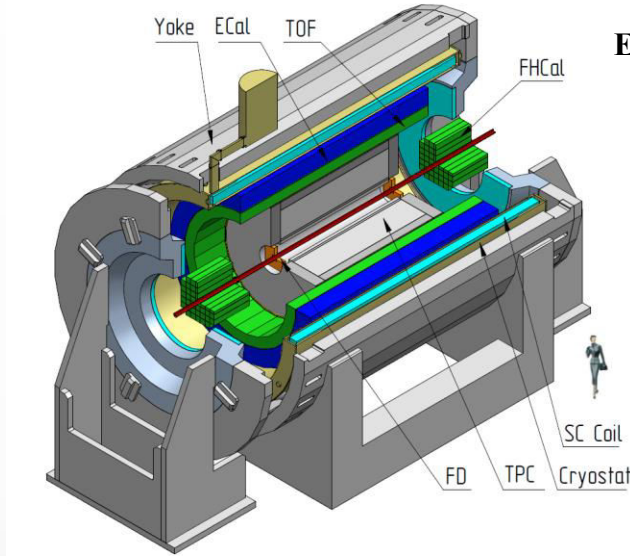
I. C. Arsene et al., Phys. Rev. C 75, 034902 (2007)

- Neutron star mergers LIGO and Virgo Collaborations, Phys. Rev. Lett. 119 (2017) 16, 161101; Nature Phys. 15 (2019) 10, 1040-1045
  - ✓ gravitational wave detection from GW170817, confirmation by astronomical observations
  - ✓  $T < 70$  MeV,  $\rho \sim 3\rho_0 \rightarrow$  about the same conditions as achieved in HIC in the laboratory
- Hyperon and hyper-nuclei measurements in HIC  $\rightarrow$  hyperon–nucleon interactions (NY, YNN)
  - ✓ key to understanding the EoS at high baryon density and inner structure of neutron stars

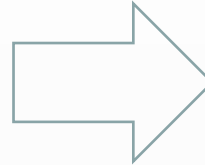
**Relativistic heavy-ion collisions provide a unique and controlled experimental way to study the properties of nuclear matter at high baryon density**

# Multi-Purpose Detector

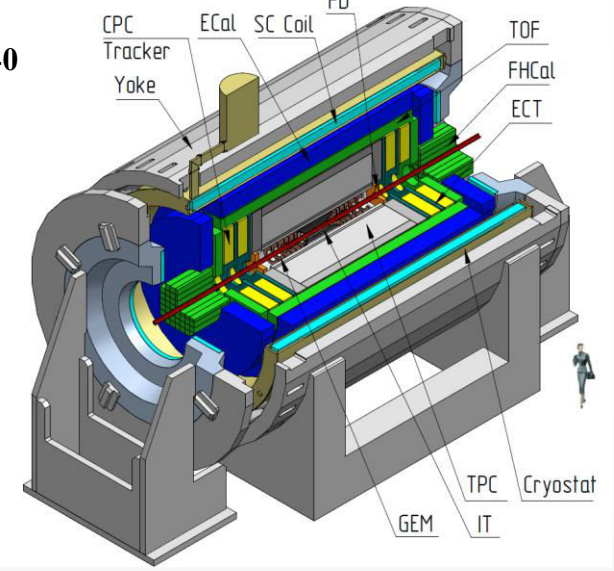
Stage-I → start of operation in 2026



Eur.Phys.J.A 58 (2022) 7, 140



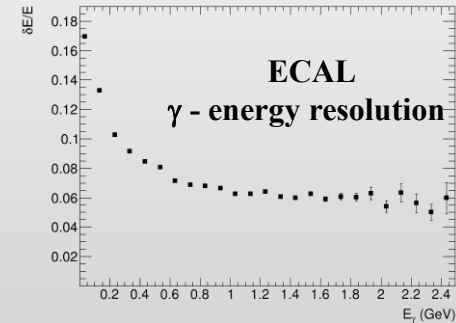
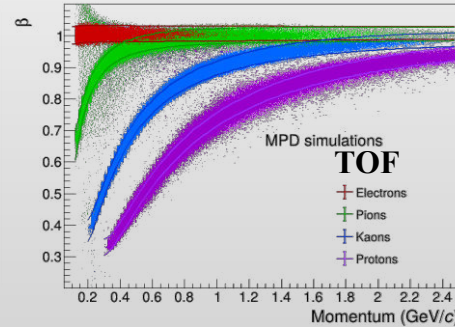
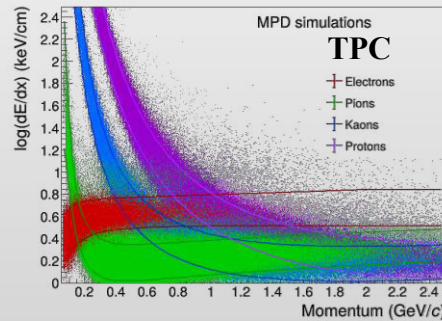
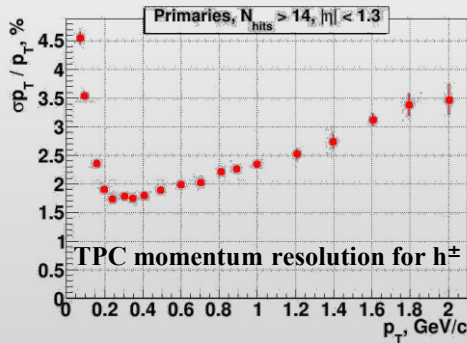
Stage-II → 2030+



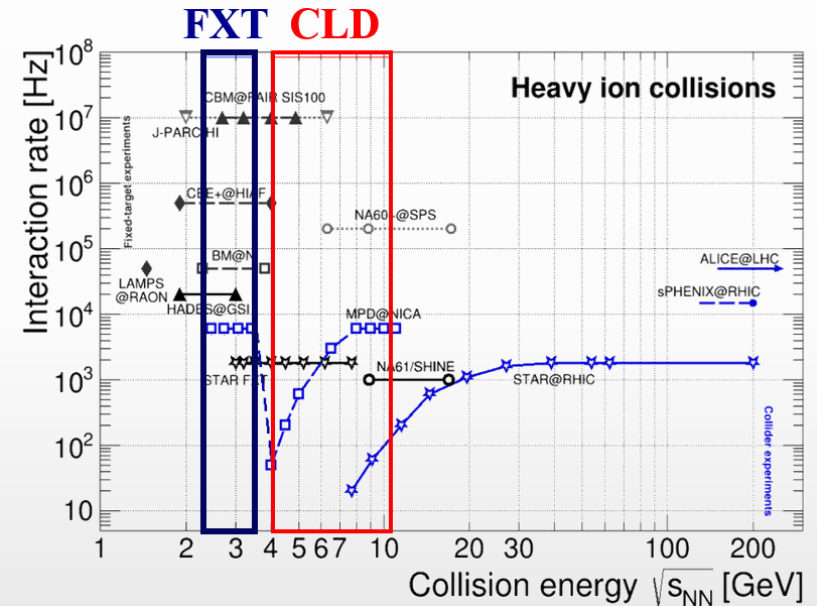
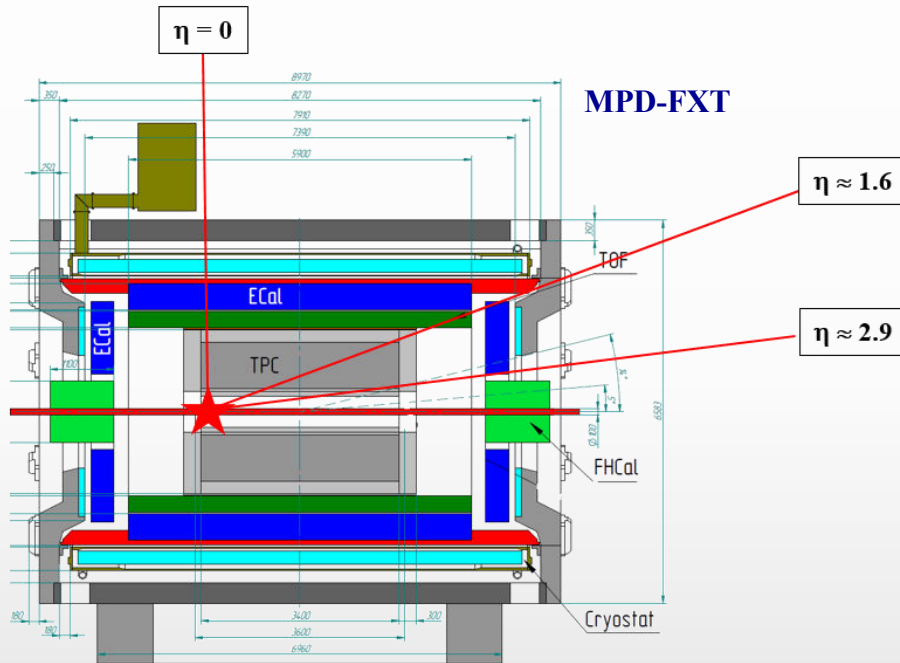
TPC:  $|\Delta\phi| < 2\pi$ ,  $|\eta| \leq 1.6$ ; TOF, EMC:  $|\Delta\phi| < 2\pi$ ,  $|\eta| \leq 1.4$   
 FFD:  $|\Delta\phi| < 2\pi$ ,  $2.9 < |\eta| < 3.3$ ; FHCAL:  $|\Delta\phi| < 2\pi$ ,  $2 < |\eta| < 5$

+ ITS :  $|\Delta\phi| < 2\pi$ ,  $|\eta| \leq 3$   
 + Forward Spectrometers:  $|\Delta\phi| < 2\pi$ ,  $|\eta| \leq 2.2$

Au+Au @ 11 GeV (full event simulation and reconstruction)



- ❖ High-luminosity scans in **energy** and **system size** to measure a wide variety of signals
- ❖ Scans to be carried out using the **same apparatus** with all the advantages of collider experiments
- ❖ MPD-CLD and MPD-FXT operation modes approved from start-up:



- ✓ Collider mode: two heavy-ion beams,  $\sqrt{s_{NN}} = 4\text{-}11$  GeV
- ✓ Fixed-target mode: one beam + thin wire as a target ( $\sim 50\text{-}100$   $\mu\text{m}$ ) :
  - extends energy range to  $\sqrt{s_{NN}} = 2.4\text{-}3.5$  GeV (overlap with HADES, BM@N, CBM)
  - high event rate at lower collision energies



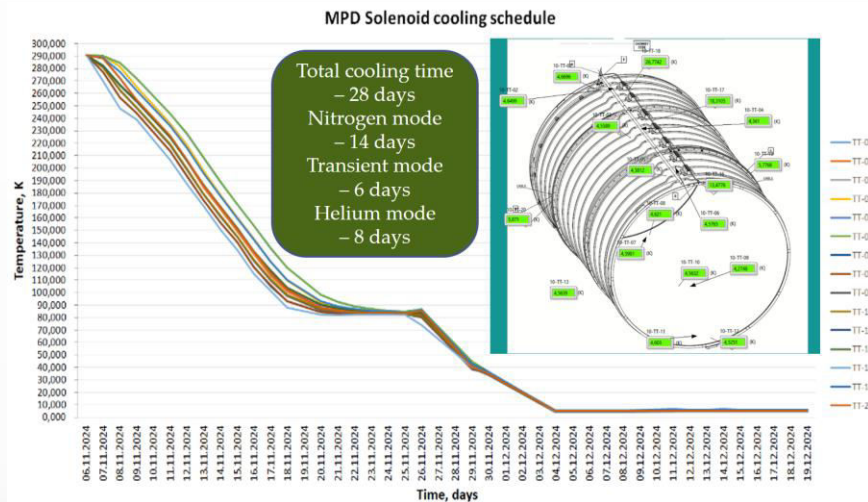
# MPD superconducting magnet

- ❖ Cooling of the magnet to LN2 and LHe temperatures → SC coil training up to 0.3 T

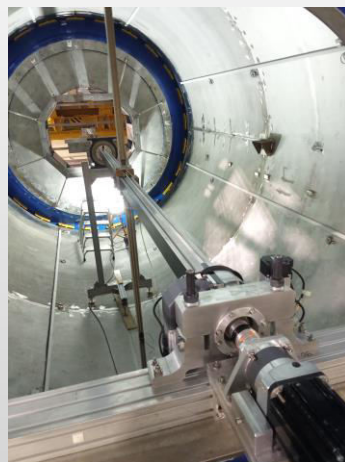
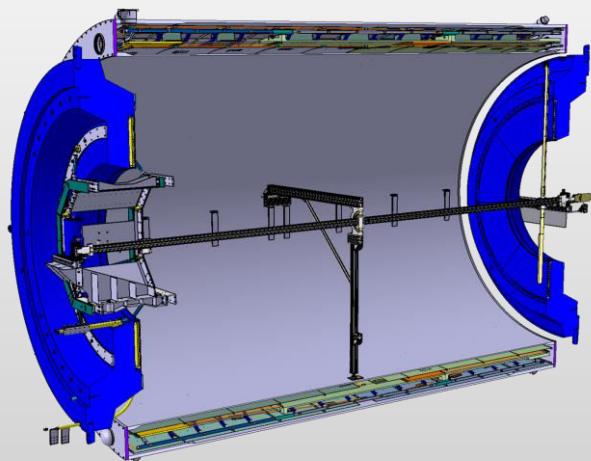
## Magnet yoke and cryogenic platform



## Cooling procedure and rate



- ❖ Magnetic field measurements: starting ...



Single 3D Hall probe moves in 3 directions:  $z$ ,  $R$ ,  $\phi$   
 Accuracy: 0.1 – 0.3 Gs  
 Number of points:  $\sim 2 \cdot 10^5$  (90 hours)  
 Fields to measure: 0.3 – 0.57 T (5-6 points)  
 Number of tunes per field: 5  
Total time of measurements:  $\sim 3$ -4 months

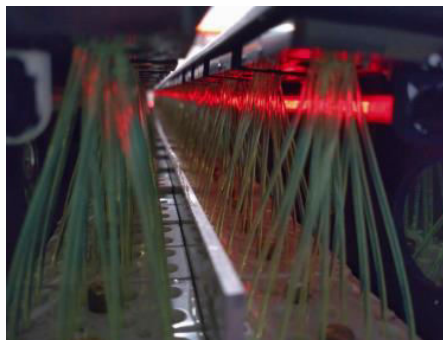
# Central barrel subsystems

## Frame - ready



Successful test installation of the carbon fiber support frame in the magnet, sagitta  $\sim 5$  mm at full load, rails for the TPC and TOF are installed

## ECAL



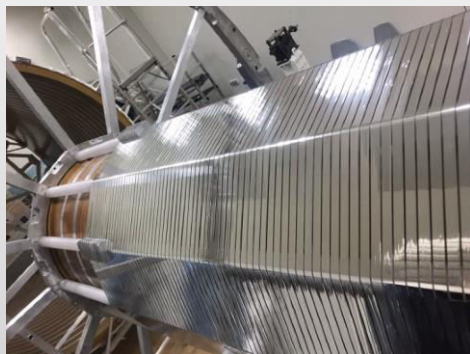
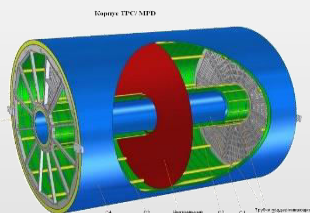
ECAL  $\sim 38400$  towers (2400 modules)  
produced by Tsinghua University, Shandong University, Fudan University, South China University, Huzhou University and JINR  
– production in IHEP (Protvino) and Tenzor (Dubna)  
45 (50 in total) half-sectors to be ready by December (April)

## TOF - ready



All 28 (100%) TOF modules are assembled, tested, stored and ready for installation.  
Spare modules in production

## TPC – central tracking detector



24+ ROC ready;  
100+ % FE cards manufactured

Ongoing TPC gas volume assembly and HV/leakage tests  
TPC + ECAL cooling systems under commissioning

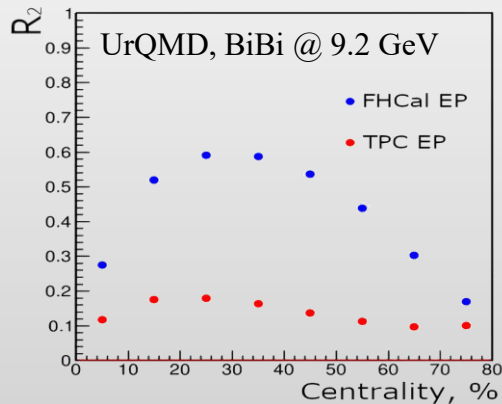


## FHCAL - ready

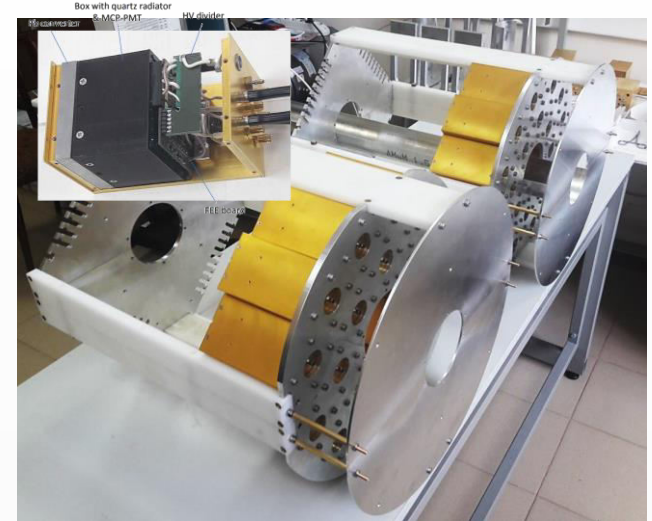


FHCAL assembled on the platform, modules are equipped with FEE and tested

FHCAL provides triggering information, centrality and event plane

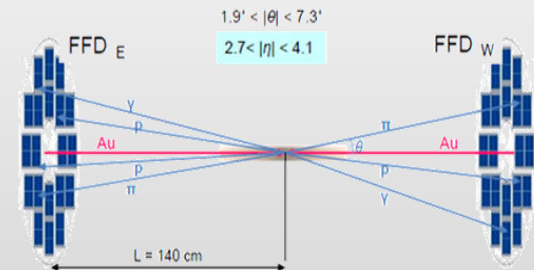


## FFD - ready



Cherenkov modules of FFDE and FFDW, mechanics for installation in container with beam pipe are available, Long term tests with cosmic rays & laser ongoing

FFD provides triggering information, even z-vertex and  $T_0$  for timing measurements



**G. Feofilov, P. Parfenov**

## **Global observables**

- Total event multiplicity
- Total event energy
- Centrality determination
- Total cross-section measurement
- Event plane measurement at all rapidities
- Spectator measurement

**V. Kireev, Xianglei Zhu**

## **Spectra of light flavor and hypernuclei**

- Light flavor spectra
- Hyperons and hypernuclei
- Total particle yields and yield ratios
- Kinematic and chemical properties of the event
- Mapping QCD Phase Diag.

**K. Mikhailov, A. Taranenko**

## **Correlations and Fluctuations**

- Collective flow for hadrons
- Vorticity,  $\Lambda$  polarization
- E-by-E fluctuation of multiplicity, momentum and conserved quantities
- Femtoscopy
- Forward-Backward corr.
- Jet-like correlations

**D. Peresunko, Chi Yang**

## **Electromagnetic probes**

- Electromagnetic calorimeter meas.
- Photons in ECAL and central barrel
- Low mass dilepton spectra in-medium modification of resonances and intermediate mass region

**Wangmei Zha, A. Zinchenko**

## **Heavy flavor**

- Study of open charm production
- Charmonium with ECAL and central barrel
- Charmed meson through secondary vertices in ITS and HF electrons
- Explore production at charm threshold

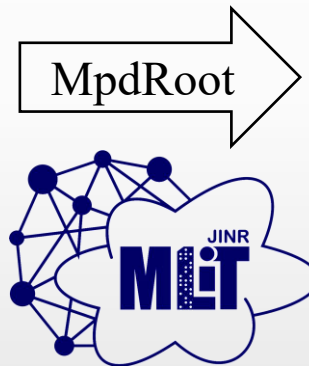
**Discuss physics feasibility studies at regular cross-PWG meetings**

- ❖ Physics feasibility studies using centralized large-scale MC productions
- ❖ Centralized Analysis Framework for access and analysis of data → Analysis Train:
  - ✓ consistent approaches and results across collaboration, easy storage and sharing of codes
  - ✓ reduced number of input/output operations for disks and databases, easier data storage on tapes
- ❖ Mescheryakov Laboratory of Information Technologies takes active participation in MPD collaboration works. We are grateful for provided computing resources, development and support of IT services.

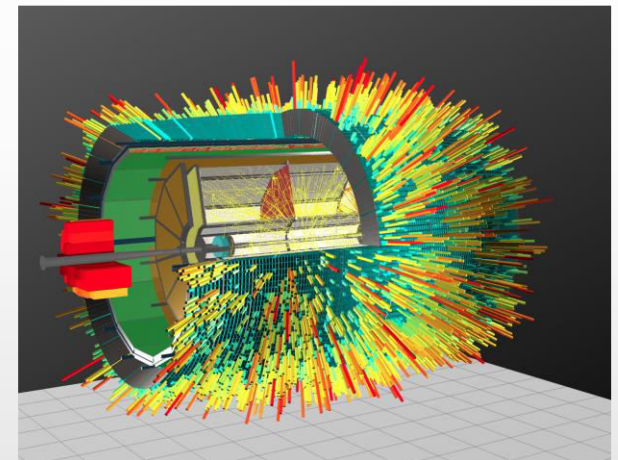
**Event generator(s)**



quarks gluons	hard scattering of partons	q,g energy loss	in-jet hadronization	hadron scattering
collision geometry		bulk expansion	bulk hadronization	



**Particle propagation & detector response**



- ❖ Develop physics program, software and analysis infrastructure for real data analysis
- ❖ MPD-CLD and MPD-FXT studies with simulations:
  - ✓ collider mode: Bi+Bi @ 9.2 GeV
  - ✓ fixed-target mode: Xe + W @ T = 2.5 AGeV



- ❖ ~ 50 reports at international conferences per year
- ❖ Overall 250+ publications indexed by SPIRES
- ❖ Collaboration papers:

## I. Status and initial physics performance studies of the MPD experiment at NICA

Eur.Phys.J.A 58 (2022) 7, 140 (~ 50 pages)

## II. MPD physics performance studies in Bi+Bi collisions at $\sqrt{s_{NN}} = 9.2$ GeV

Rev.Mex.Fis. 71 (2025) 4, 041201, e-Print: 2503.21117 (~ 40 pages)

Eur. Phys. J. A manuscript No.  
(will be inserted by the editor)

## Status and initial physics performance studies of the MPD experiment at NICA

The MPD Collaboration

<sup>1</sup>The full list of Collaboration Members is provided at the end of the manuscript.

Received: April 20, 2022/ Accepted: date

<b>Abstract</b>	<b>The nucleon-based Ion Collider Facility (NICA)</b>	<b>1.1 The Joint "Fragment" System</b>	22
	NICA is under construction at the Joint Institute for Nuclear Research (JINR), with commissioning of the facility expected in late 2022. The <b>High-Purpose Ion Collider (MPD)</b> has been designed to operate at NICA and its components are currently in production. The detector is expected to be ready for data taking with the first beams from NICA. This document provides an overview of the landscape of the investigation of the QCD phase diagram in the region of maximum baryonic density, where NICA and MPD will be able to provide significant and unique input. It also provides a detailed description of the MPD set-up, including its various subsystems as well as its support and computing infrastructure. Selected performance studies for particular physics measurements at MPD are presented and discussed in the context of existing data and theoretical expectations.	<b>1.2 The Ion-Mixing Experiment</b>	23
		<b>1.3 The Cosmic-Ray Ion Experiment</b>	24
		<b>1.4 The Heavy-Ion Experiment</b>	25
		<b>1.5 MPD</b>	26
		<b>1.6 The Ion-Beam Transport</b>	27
		<b>1.7 Support system</b>	28
		<b>1.8 Beam Diagnostics</b>	29
		<b>1.9 Slow Control System</b>	30
		<b>1.10 Data Acquisition</b>	31
		<b>Software development and computing resources for NICA</b>	32
		<b>2.1 Software</b>	33
		<b>2.2 Hardware</b>	34
		<b>2.3 Performance for data taking</b>	35
		<b>Examples of physics feasibility studies</b>	36
		<b>3.1 Heavy-ion collisions</b>	37
		<b>3.2 High-pseudrapidity nuclear spectra, yields and ratios</b>	38
		<b>3.3 High-pseudrapidity nuclear spectra, yields and ratios</b>	39
		<b>3.4 A and <math>\bar{A}</math> and <math>2A</math> and <math>2\bar{A}</math> reconstruction</b>	40
		<b>3.5 <math>2A</math> and <math>2\bar{A}</math> reconstruction</b>	41
		<b>3.6 <math>2A</math> and <math>2\bar{A}</math> reconstruction</b>	42
		<b>3.7 Electromagnetic probes</b>	43
		<b>3.8 Electromagnetic probes</b>	44
		<b>3.9 Electromagnetic probes and nuclear structure</b>	45
		<b>3.10 Electromagnetic probes and nuclear structure</b>	46
		<b>3.11 Electromagnetic probes and nuclear structure</b>	47
		<b>3.12 Electromagnetic probes and nuclear structure</b>	48
		<b>3.13 Electromagnetic probes and nuclear structure</b>	49
		<b>3.14 Electromagnetic probes and nuclear structure</b>	50
		<b>3.15 Electromagnetic probes and nuclear structure</b>	51
		<b>3.16 Electromagnetic probes and nuclear structure</b>	52
		<b>3.17 Electromagnetic probes and nuclear structure</b>	53
		<b>3.18 Electromagnetic probes and nuclear structure</b>	54
		<b>3.19 Electromagnetic probes and nuclear structure</b>	55
		<b>3.20 Electromagnetic probes and nuclear structure</b>	56
		<b>3.21 Electromagnetic probes and nuclear structure</b>	57
		<b>3.22 Electromagnetic probes and nuclear structure</b>	58
		<b>3.23 Electromagnetic probes and nuclear structure</b>	59
		<b>3.24 Electromagnetic probes and nuclear structure</b>	60
		<b>3.25 Electromagnetic probes and nuclear structure</b>	61
		<b>3.26 Electromagnetic probes and nuclear structure</b>	62
		<b>3.27 Electromagnetic probes and nuclear structure</b>	63
		<b>3.28 Electromagnetic probes and nuclear structure</b>	64
		<b>3.29 Electromagnetic probes and nuclear structure</b>	65
		<b>3.30 Electromagnetic probes and nuclear structure</b>	66
		<b>3.31 Electromagnetic probes and nuclear structure</b>	67
		<b>3.32 Electromagnetic probes and nuclear structure</b>	68
		<b>3.33 Electromagnetic probes and nuclear structure</b>	69
		<b>3.34 Electromagnetic probes and nuclear structure</b>	70
		<b>3.35 Electromagnetic probes and nuclear structure</b>	71
		<b>3.36 Electromagnetic probes and nuclear structure</b>	72
		<b>3.37 Electromagnetic probes and nuclear structure</b>	73
		<b>3.38 Electromagnetic probes and nuclear structure</b>	74
		<b>3.39 Electromagnetic probes and nuclear structure</b>	75
		<b>3.40 Electromagnetic probes and nuclear structure</b>	76
		<b>3.41 Electromagnetic probes and nuclear structure</b>	77
		<b>3.42 Electromagnetic probes and nuclear structure</b>	78
		<b>3.43 Electromagnetic probes and nuclear structure</b>	79
		<b>3.44 Electromagnetic probes and nuclear structure</b>	80
		<b>3.45 Electromagnetic probes and nuclear structure</b>	81
		<b>3.46 Electromagnetic probes and nuclear structure</b>	82
		<b>3.47 Electromagnetic probes and nuclear structure</b>	83
		<b>3.48 Electromagnetic probes and nuclear structure</b>	84
		<b>3.49 Electromagnetic probes and nuclear structure</b>	85
		<b>3.50 Electromagnetic probes and nuclear structure</b>	86
		<b>3.51 Electromagnetic probes and nuclear structure</b>	87
		<b>3.52 Electromagnetic probes and nuclear structure</b>	88
		<b>3.53 Electromagnetic probes and nuclear structure</b>	89
		<b>3.54 Electromagnetic probes and nuclear structure</b>	90
		<b>3.55 Electromagnetic probes and nuclear structure</b>	91
		<b>3.56 Electromagnetic probes and nuclear structure</b>	92
		<b>3.57 Electromagnetic probes and nuclear structure</b>	93
		<b>3.58 Electromagnetic probes and nuclear structure</b>	94
		<b>3.59 Electromagnetic probes and nuclear structure</b>	95
		<b>3.60 Electromagnetic probes and nuclear structure</b>	96
		<b>3.61 Electromagnetic probes and nuclear structure</b>	97
		<b>3.62 Electromagnetic probes and nuclear structure</b>	98
		<b>3.63 Electromagnetic probes and nuclear structure</b>	99
		<b>3.64 Electromagnetic probes and nuclear structure</b>	100
		<b>3.65 Electromagnetic probes and nuclear structure</b>	101
		<b>3.66 Electromagnetic probes and nuclear structure</b>	102
		<b>3.67 Electromagnetic probes and nuclear structure</b>	103
		<b>3.68 Electromagnetic probes and nuclear structure</b>	104
		<b>3.69 Electromagnetic probes and nuclear structure</b>	105
		<b>3.70 Electromagnetic probes and nuclear structure</b>	106
		<b>3.71 Electromagnetic probes and nuclear structure</b>	107
		<b>3.72 Electromagnetic probes and nuclear structure</b>	108
		<b>3.73 Electromagnetic probes and nuclear structure</b>	109
		<b>3.74 Electromagnetic probes and nuclear structure</b>	110
		<b>3.75 Electromagnetic probes and nuclear structure</b>	111
		<b>3.76 Electromagnetic probes and nuclear structure</b>	112
		<b>3.77 Electromagnetic probes and nuclear structure</b>	113
		<b>3.78 Electromagnetic probes and nuclear structure</b>	114
		<b>3.79 Electromagnetic probes and nuclear structure</b>	115
		<b>3.80 Elect</b>	

Nuclear Physics

Revista Mexicana de Física 71 041201 1-45

JULY-AUGUST 2021

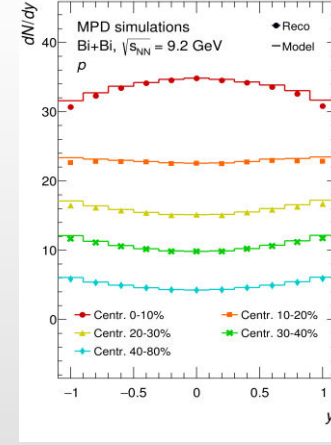
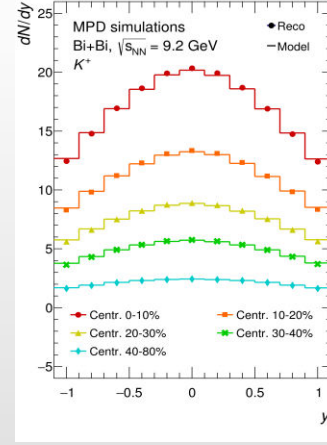
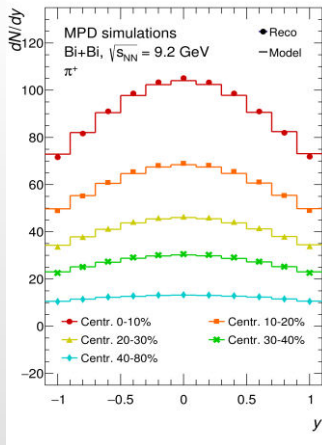
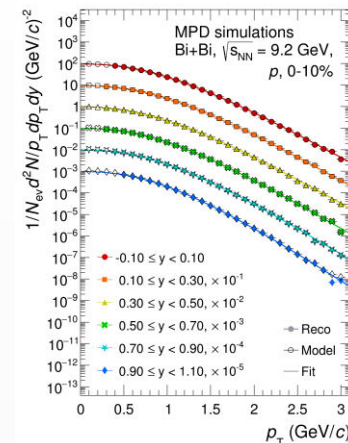
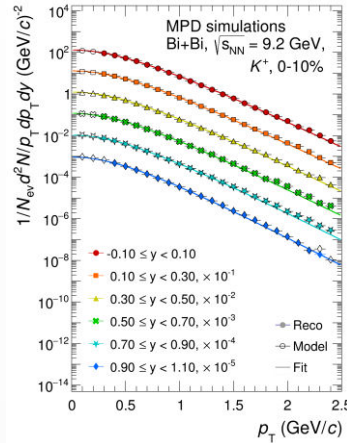
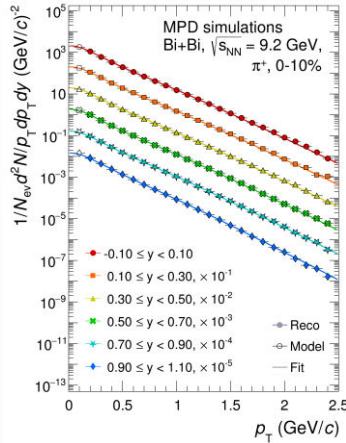
MPD physics performance studies in Bi+Bi collisions at  $\sqrt{s_{NN}} = 9.2$  GeV[illegible]

# Light identified hadrons

- ✓ probe freeze-out conditions
- ✓ radial flow and collective expansion
- ✓ hadronization mechanisms, thermal models vs. coalescence
- ✓ strangeness production, “horn” for  $K/\pi$ , hidden strangeness with  $\phi(1020)$
- ✓ lifetime and properties of the late hadronic phase
- ✓ fluctuation of net-baryon (proton) and net-strangeness (kaon) numbers
- ✓ parton energy loss
- ✓ ...

# Charged hadrons, Bi + Bi @ 9.2 GeV

❖ Charged hadrons: large and uniform acceptance + excellent PID capabilities of TPC and TOF



Cover ( $p_T$  - rapidity) phase space corresponding to  $\sim 70\%$  of  $\pi/K/p$  total production

Cover  $p_T$  range that corresponds to  $> 90\%$  of  $\pi/K/p$  total production at midrapidity  $\rightarrow$  small unc. for  $dN/dy$

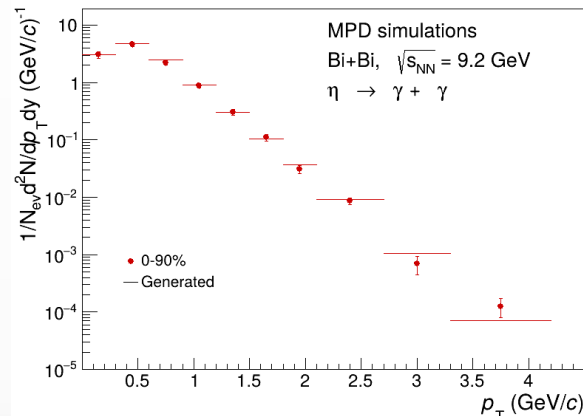
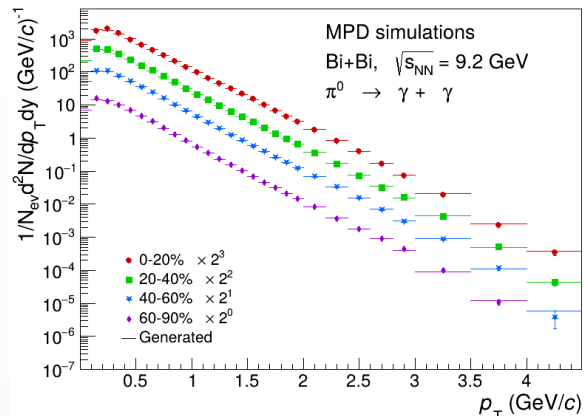
Wide  $p_T$  coverage for combined Blast-Wave fits  $\rightarrow \beta, T_{kin}$



## ❖ Neutral mesons:

✓  $\pi^0/\eta \rightarrow \gamma\gamma$ ,  $\pi^0/\eta \rightarrow \gamma(e^+e^-)$ ,  $\pi^0/\eta \rightarrow (e^+e^-)(e^+e^-)$ ;  $K_s \rightarrow \pi^0\pi^0$ ;  $\omega \rightarrow \pi^0\gamma$ ,  $\omega/\eta \rightarrow \pi^0\pi^+\pi^-$ ;  $\eta' \rightarrow \eta\pi^+\pi^-$

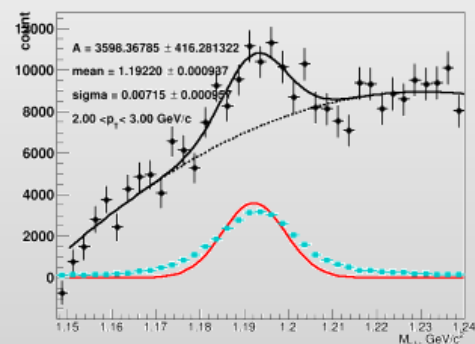
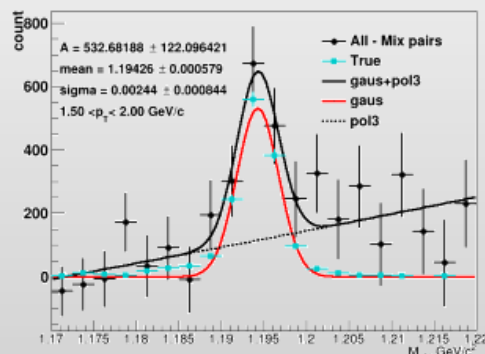
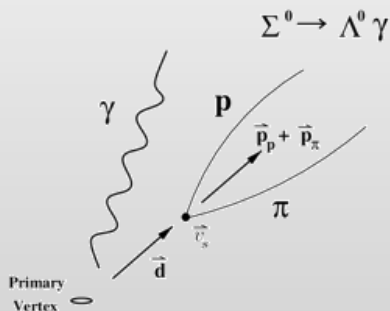
## ❖ Photons: ECAL reconstruction + photon conversion method (PCM)



Extended  $p_T$  ranges compared to charged particle measurements

Different systematics and species (masses, quark contents)

## ❖ ... and event baryons: $\Sigma^0 \rightarrow \Lambda\gamma$ , $\Sigma^0 \rightarrow \Lambda(e^+e^-)$ , $\Sigma^+ \rightarrow p\pi^0$



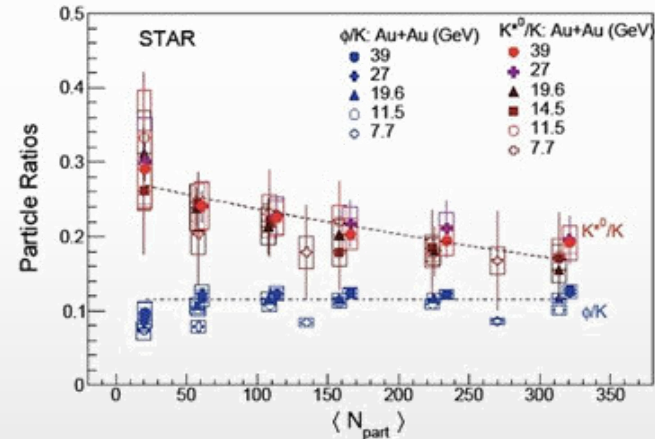
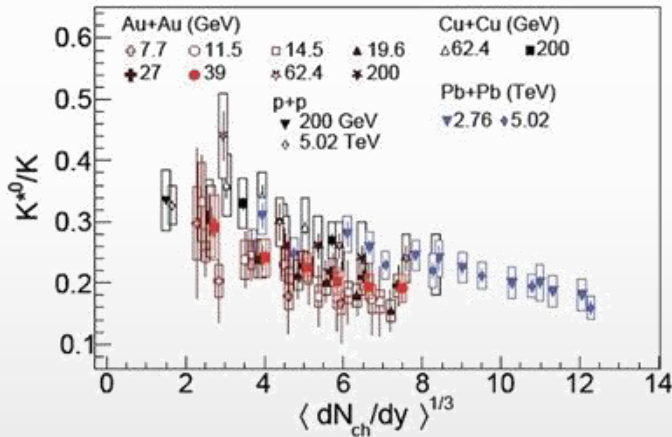
# Hadronic resonances

- ❖ Resonances probe reaction dynamics and particle production mechanisms vs. system size and  $\sqrt{s_{NN}}$ :
  - ✓ strangeness production, lifetime and properties of the hadronic phase, spin alignment of vector mesons, flow etc.

increasing lifetime  $\longrightarrow$

	$\rho(770)$	$K^*(892)$	$\Sigma(1385)$	$\Lambda(1520)$	$\Xi(1530)$	$\phi(1020)$
$c\tau$ (fm/c)	1.3	4.2	5.5	12.7	21.7	46.2
$\sigma_{\text{rescatt}}$	$\sigma_{\pi}\sigma_{\pi}$	$\sigma_{\pi}\sigma_K$	$\sigma_{\pi}\sigma_{\Lambda}$	$\sigma_K\sigma_p$	$\sigma_{\pi}\sigma_{\Xi}$	$\sigma_K\sigma_K$

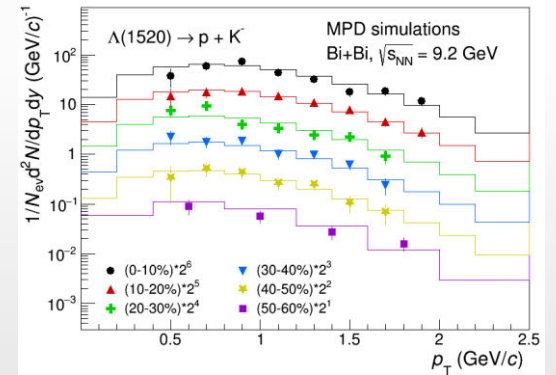
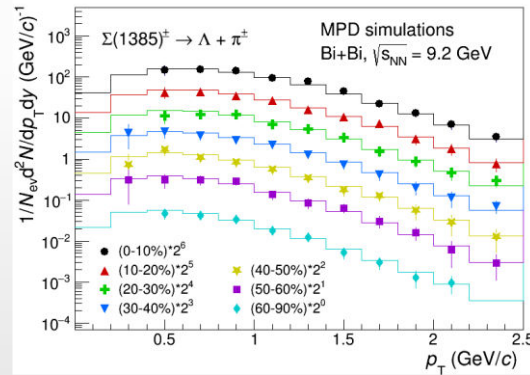
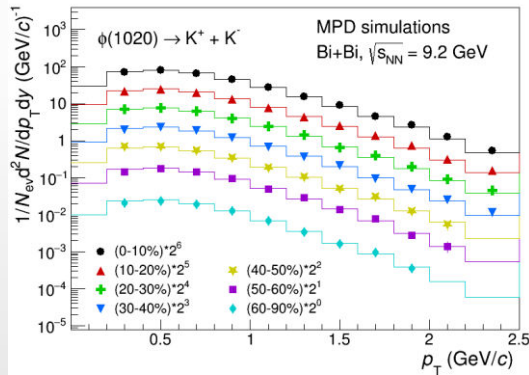
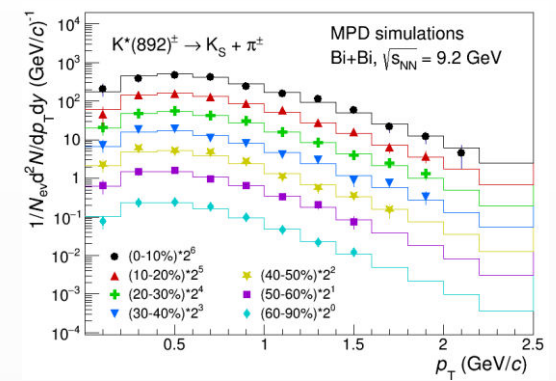
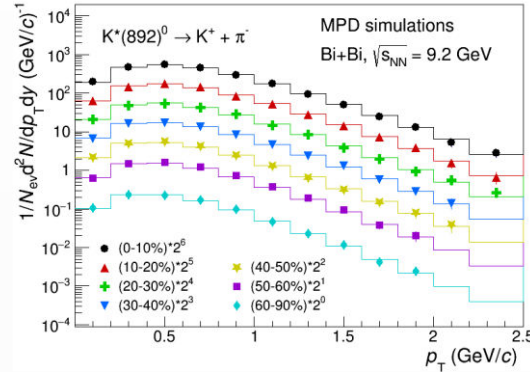
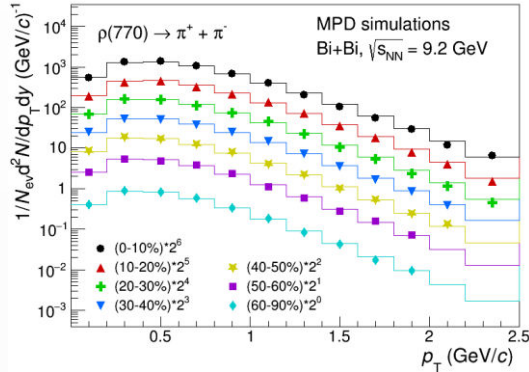
- ❖ Properties of the hadronic phase are studied by measuring ratios of resonance yields to yields of long-lived particles with same/similar quark contents:  $\rho/\pi$ ,  $K^*/K$ ,  $\phi/K$ ,  $\Lambda^*/\Lambda$ ,  $\Sigma^{*\pm}/\Sigma$  and  $\Xi^{*0}/\Xi$



- ❖ Suppression of the ratios for shorter-lived resonances is explained by the existence of a hadronic phase that lives long enough (up to  $\tau \sim 10$  fm/c) to cause a significant reduction of the reconstructed yields  $\rightarrow$  present at NICA confirmed by measurements and transport model (UrQMD) calculations

**Precise measurements at NICA are needed to validate description of the hadronic phase in models**

❖ PID capabilities of TPC and TOF + topology selections for weak decays of daughters ( $K_S$ ,  $\Lambda$ )



A wide variety of resonances is constructible,  $\rho(770)$ ,  $K^*(892)$ ,  $\phi(1020)$ ,  $\Sigma(1385)$ ,  $\Lambda(1520)$

Measurements are possible starting from  $\sim$  zero momentum  $\rightarrow$  sample most of the yields

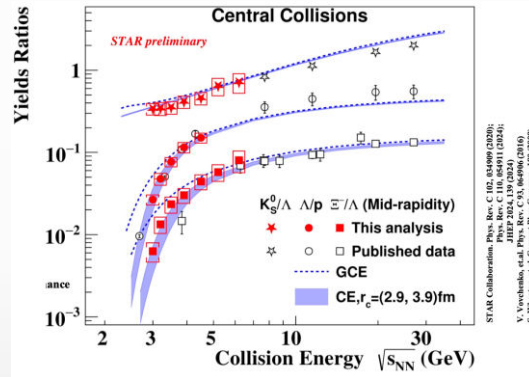
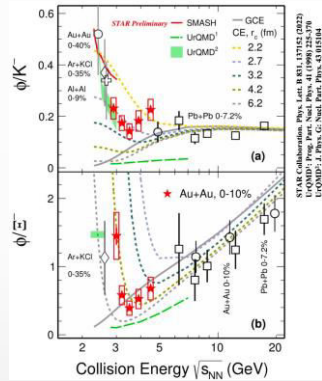
Angular dependent measurements with larger statistics  $\rightarrow$  spin alignment, collective flow



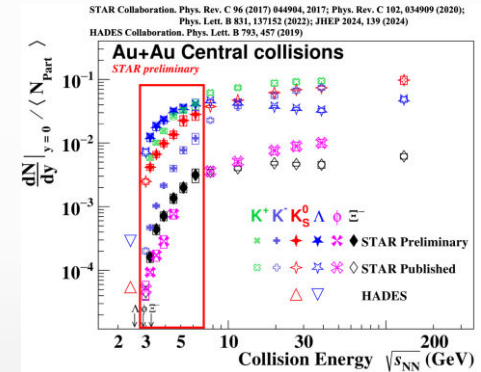
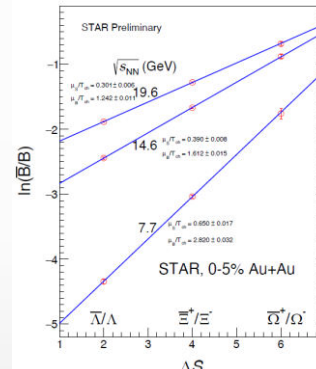
## **(Multi)strange baryons**

# Strangeness production

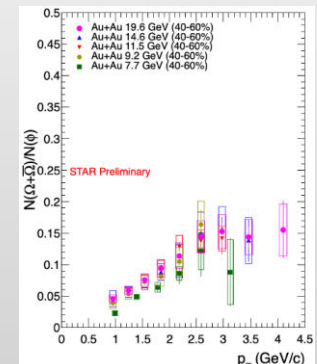
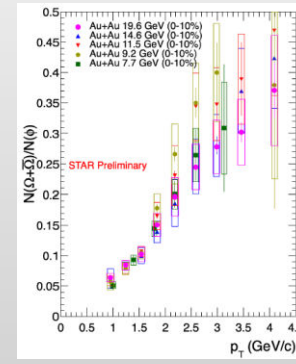
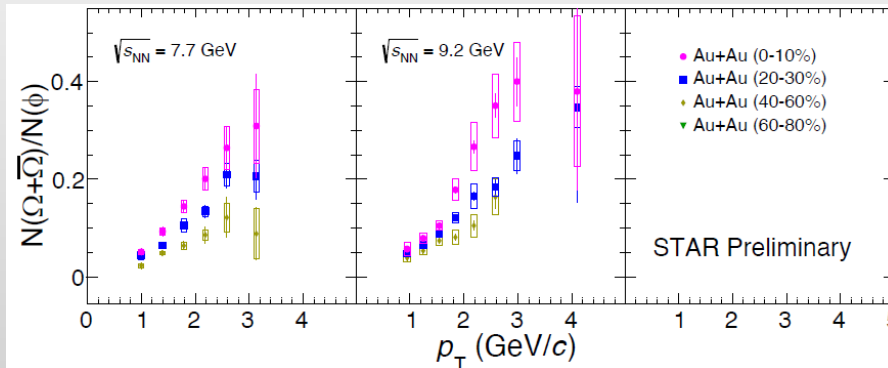
- ❖ Small hadronic cross-sections  
→ sensitivity to early stages of medium dynamics
- ❖ Yields of strange hadrons (low  $p_T$ )  
→ strangeness enhancement, proposed as a signature of QGP since 80's, now described by statistical/thermal models  
→ information about chemical freeze-out parameters  
→ near or sub-threshold production



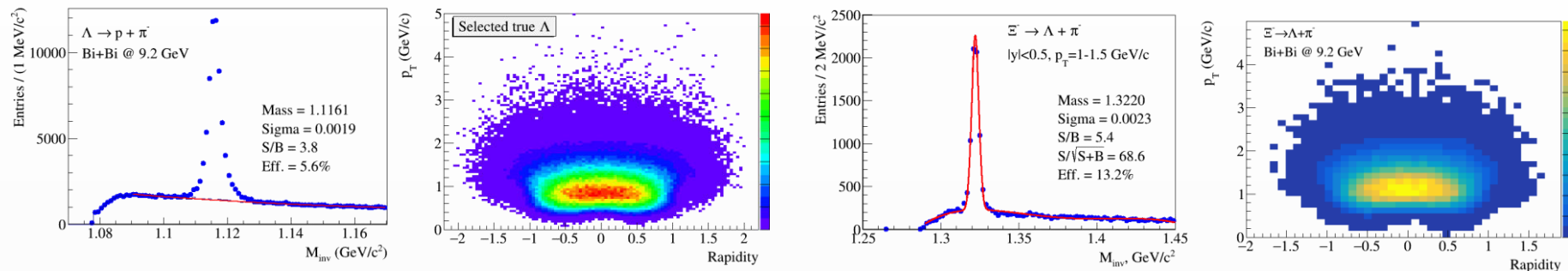
$$\ln(\bar{B}/B) = -2\mu_B/T_{ch} + \mu_S/T_{ch}\Delta S$$



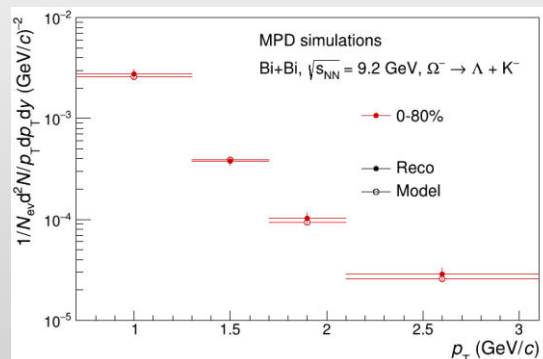
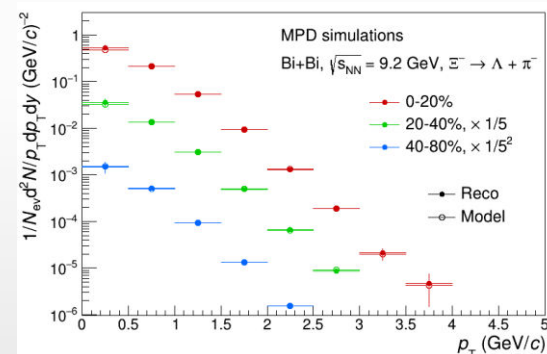
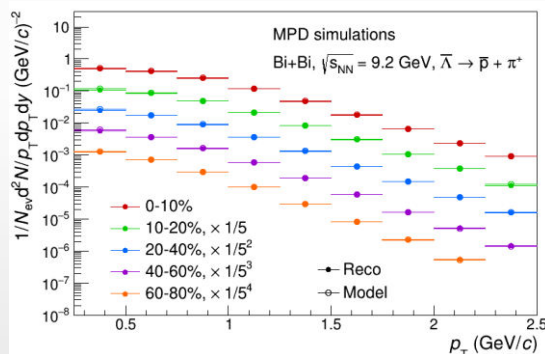
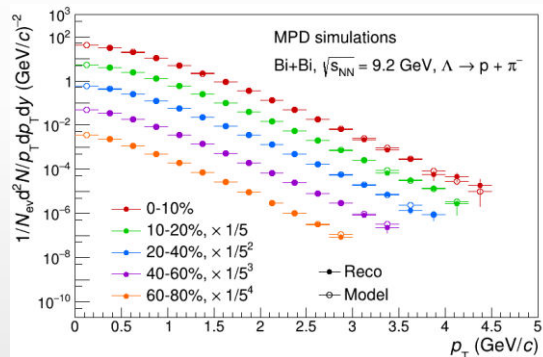
- ❖ Hyperon-to-meson ratios vs.  $p_T$  (intermediate  $p_T$ )  
→ hadronization with parton coalescence, freeze-out conditions



## ❖ PID capabilities of TPC and TOF + topology selections



- different background estimates (fit function vs mixed-event), testing alternative Machine Learning techniques

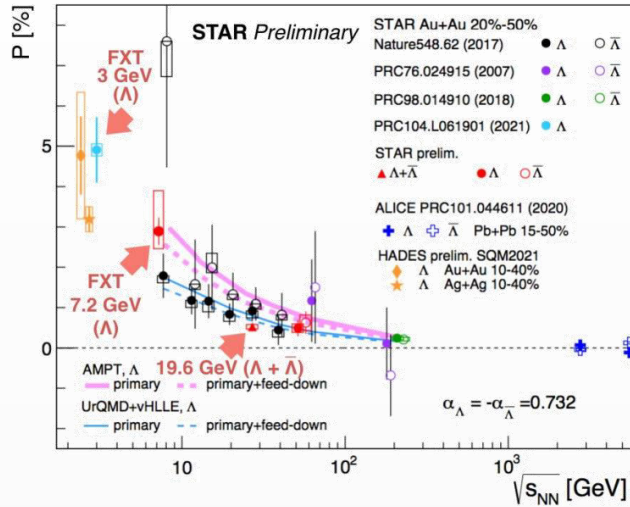


**MPD has capabilities to measure production of strange charged/neutral kaons, (multi)strange baryons and resonances in pp, p-A and A-A collisions using h-ID in the TPC&TOF and different decay topology selections**



# Global polarization

- ❖ Global polarization of hyperons experimentally observed, decreases with  $\sqrt{s_{NN}}$



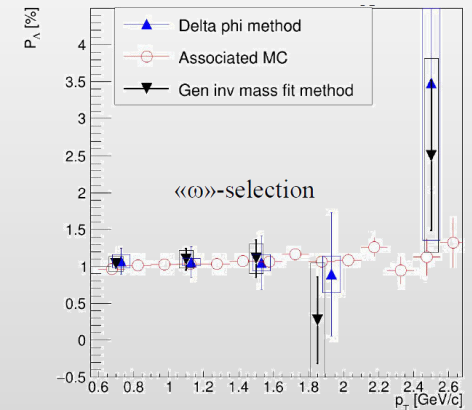
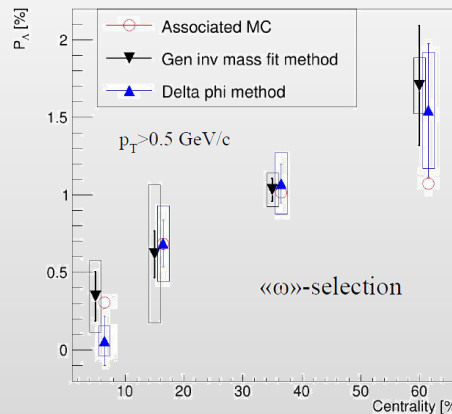
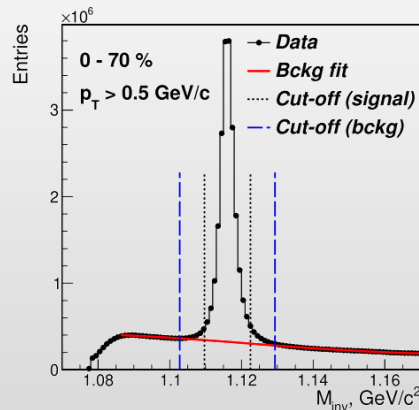
- ✓ reproduced by AMPT, 3FD, UrQMD+VHLL
- ✓ hint for a  $\Lambda$ - $\bar{\Lambda}$  difference, magnetic field:

$$P_{\Lambda} \simeq \frac{1}{2} \frac{\omega}{T} + \frac{\mu_{\Lambda} B}{T} \quad P_{\bar{\Lambda}} \simeq \frac{1}{2} \frac{\omega}{T} - \frac{\mu_{\Lambda} B}{T}$$

**NICA: extra points in the energy range 2-11 GeV centrality,  $p_T$  and rapidity dependence of polarization, not only for  $\Lambda$ , but other (anti)hyperons ( $\Lambda$ ,  $\Sigma$ ,  $\Xi$ )**

- ❖ MPD performance: BiBi@9.2 GeV (PHSD, 15 M events)  $\rightarrow$  full reconstruction  $\rightarrow$   $\Lambda$  global polarization

Performance study of the hyperon global polarization measurements with MPD at NICA, Eur.Phys.J.A 60 (2024) 4, 85

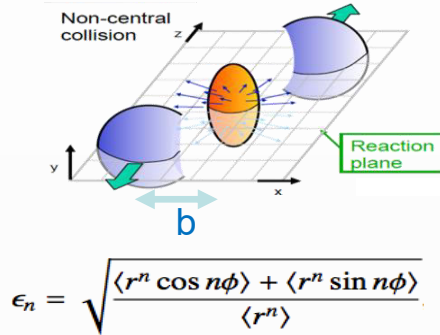


**MPD: first global polarization measurements for  $\Lambda/\bar{\Lambda}$  will be possible with  $\sim 20$ M data sampled events**

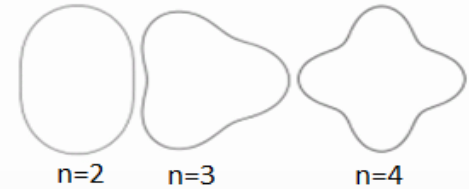
## Collective flow

- ❖ Initial eccentricity and its fluctuations drive momentum anisotropy  $v_n$  with specific viscous modulation

Spatial anisotropy of the nuclear overlap region



Azimuthal distribution of produced particles wrt to reaction plane ( $\Psi_n$ )

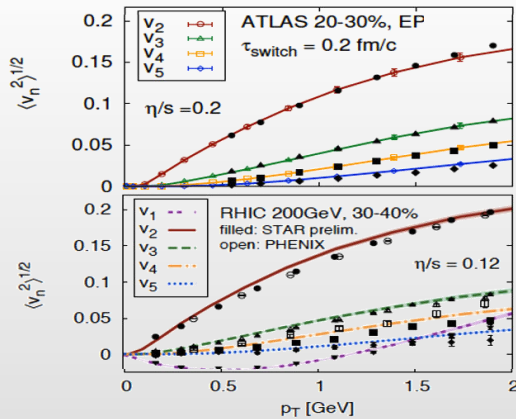


$$\frac{dN}{d\phi} \propto \left( 1 + 2 \sum_{n=1} v_n \cos[n(\phi - \Psi_n)] \right)$$

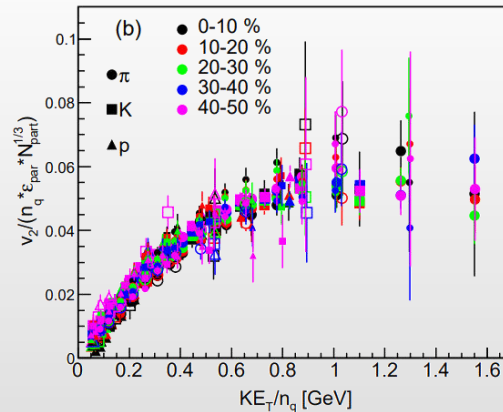
Anisotropic flow:  $v_n = \langle \cos[n(\phi - \Psi_n)] \rangle$

- ❖ Evidence for a dense perfect liquid found at RHIC/LHC (M. Roizard et al., Scientific American, 2006)

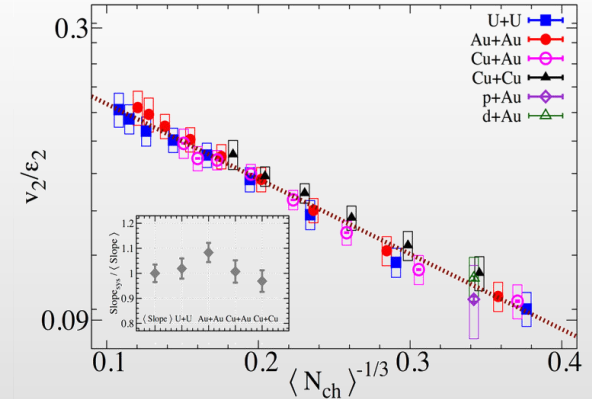
Gale, Jeon et al., Phys. Rev. Lett. 110, 012302



Phys.Rev.C 92 (2015) 3, 034913



Phys. Rev. Lett. 122 (2019) 172301



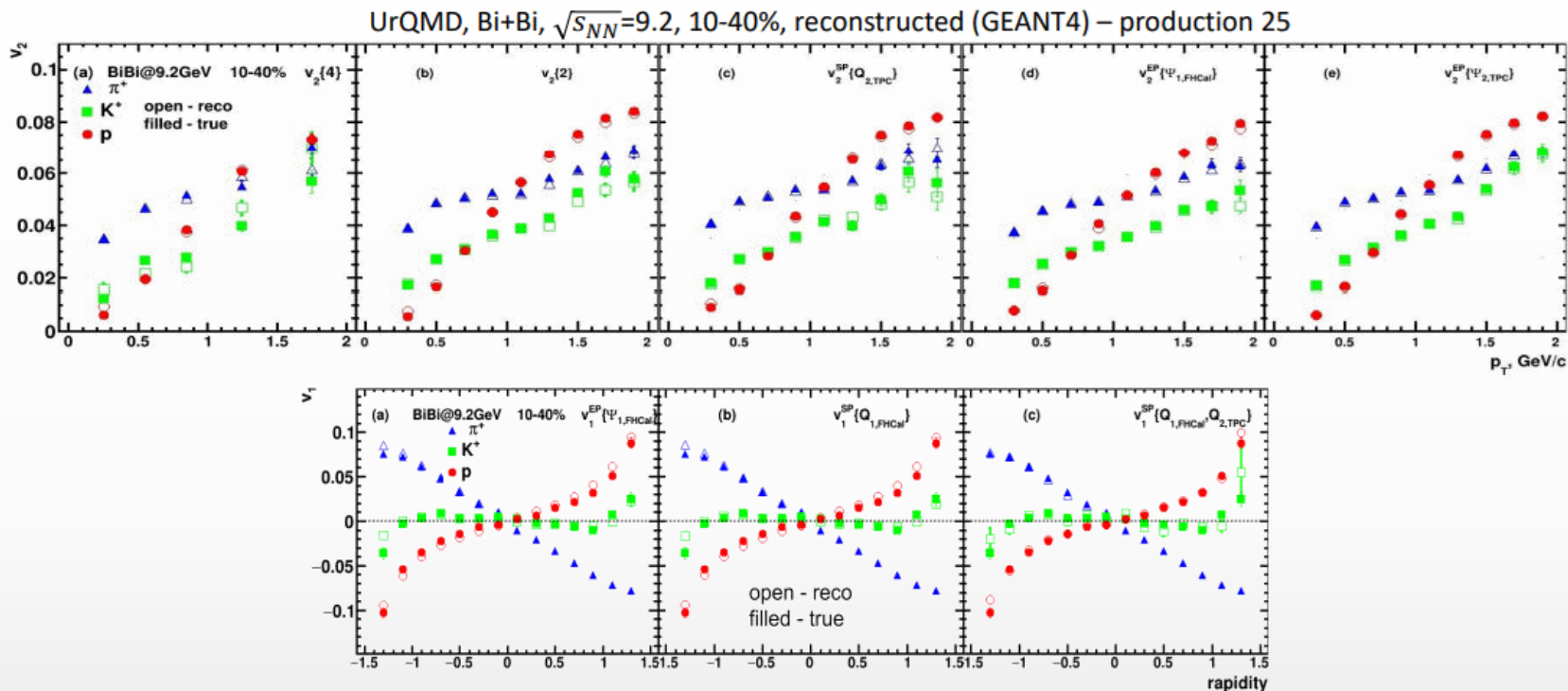
**System size scan (p-A, A-A) is an important ingredient:**

initial geometry  $\rightarrow$  flow harmonics  $\rightarrow \frac{\eta}{s}(T, \mu), \frac{\zeta}{s}(T, \mu), c_s(T), \alpha_s(T), etc.$



# MPD performance for $v_1, v_2$ of $\pi/K/p$

❖ BiBi@9.2 GeV (UrQMD, 50M), full event reconstruction



❖ Reconstructed and generated  $v_1$  and  $v_2$  for identified hadrons are in good agreement for all methods

**MPD has capabilities to measure different flow harmonics for a wide variety of identified hadrons**

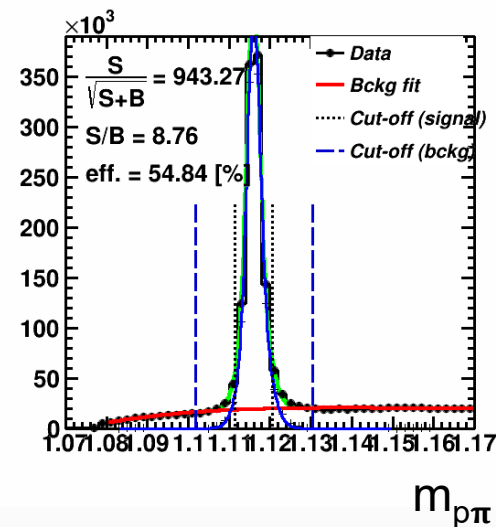
**System size scan for flow measurements is vital for understanding of the medium transport properties and onset of the phase transition**

❖ BiBi@9.2 GeV (PHSD, 15M), full event reconstruction

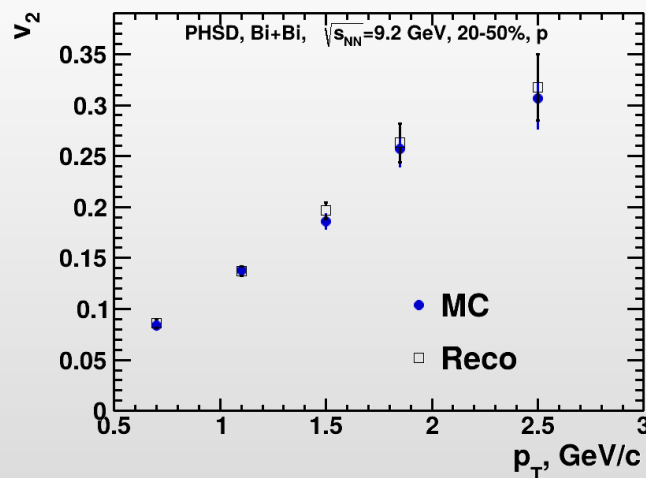
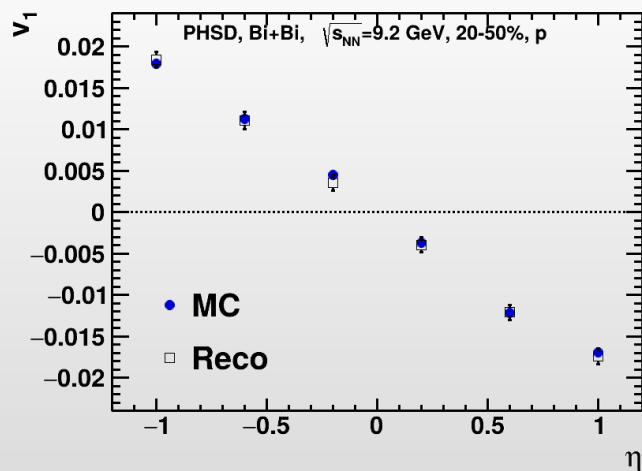
Differential flow can be defined using the following fit:

$$v_n^{SB}(m_{inv}) = v_n^S \frac{N^S(m_{inv})}{N^{SB}(m_{inv})} + v_n^B(m_{inv}) \frac{N^B(m_{inv})}{N^{SB}(m_{inv})}$$

- $v_n^S$  - signal anisotropic flow (set as a parameter in the fit)
- $v_n^B(m_{inv})$  - background flow (set as polynomial function)



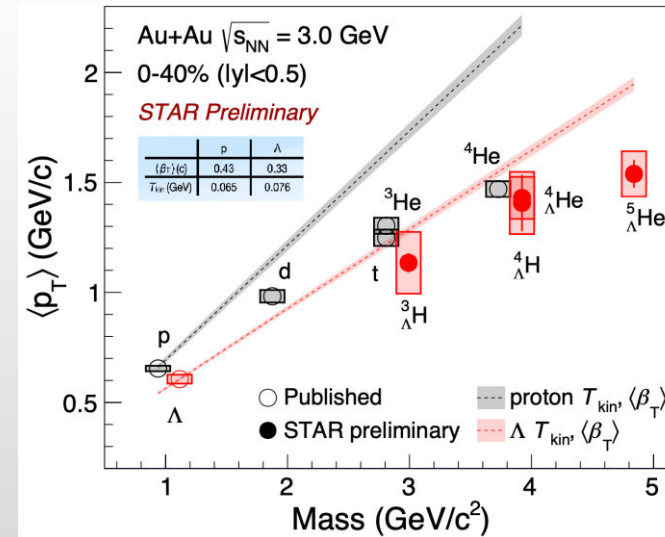
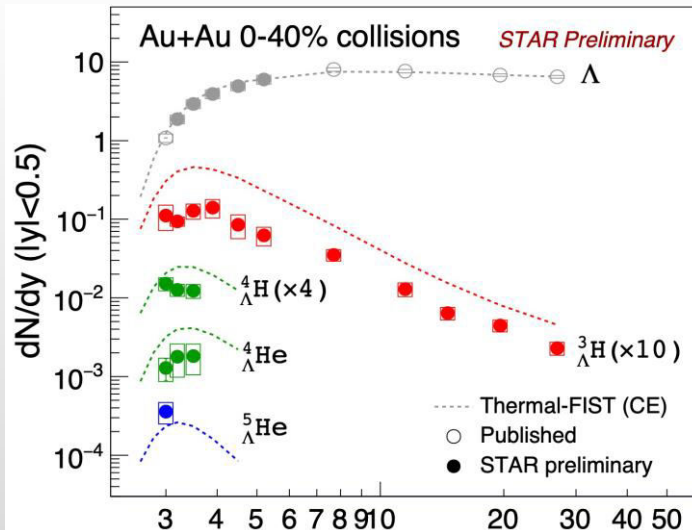
❖ Performance of  $v_1$  and  $v_2$  of  $\Lambda$  hyperons:



- ❖ Good performance for  $v_1$ ,  $v_2$  using invariant mass fit and event plane methods
- ❖ Similar measurements for Ks, other hyperons and short-lived resonances

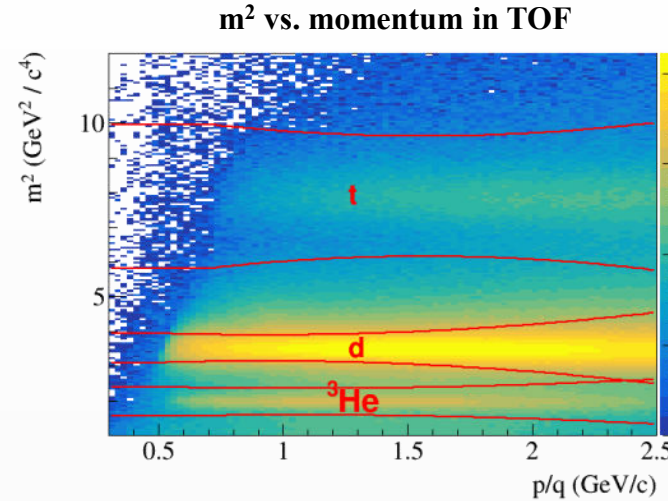
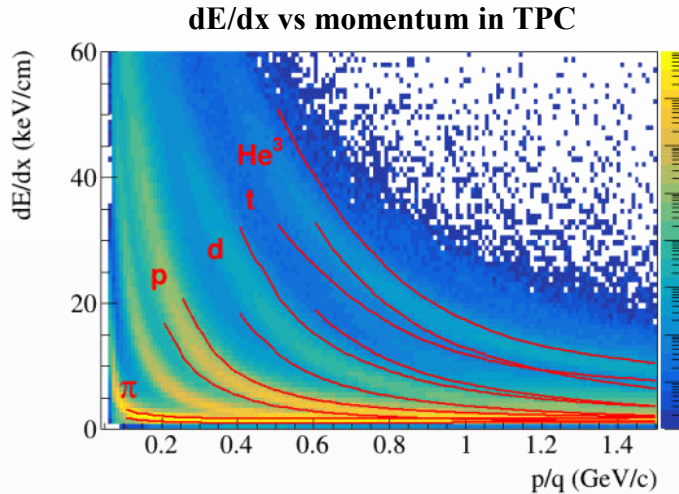
# Light (hyper)nuclei

- ❖ Production mechanism usually described with two classes of phenomenological models :
  - ✓ statistical hadronization (SHM)  $\rightarrow$  production during phase transition,  $dN/dy \propto \exp(-m/T_{\text{chem}})$  [1]
  - ✓ coalescence  $\rightarrow$  (anti)nucleons close in phase space ( $\Delta p < p_0$ ) and matching the spin state form a nucleus [2]
- ❖ Hyper nuclei measurement studies are crucial:
  - ✓ microscopic production mechanism, Y-N potential, strange sector of nuclear EoS
  - ✓ strong implications for astrophysics  $\rightarrow$  hyperons expected to exist in the inner core of neutron stars
- ❖ Models predict enhanced hypernuclear production at NICA energies  $\rightarrow$  offers great opportunity for hypernuclei measurements in MPD, double hypernuclei may be reachable
- ❖ Observables of interest: binding energies, lifetimes, branching ratios,  $\langle p_T \rangle$ ,  $dN/dy$

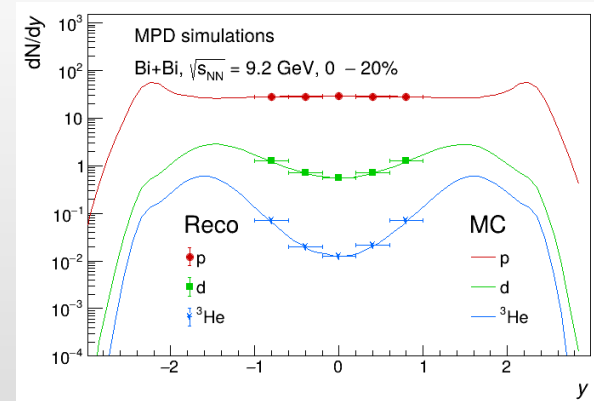
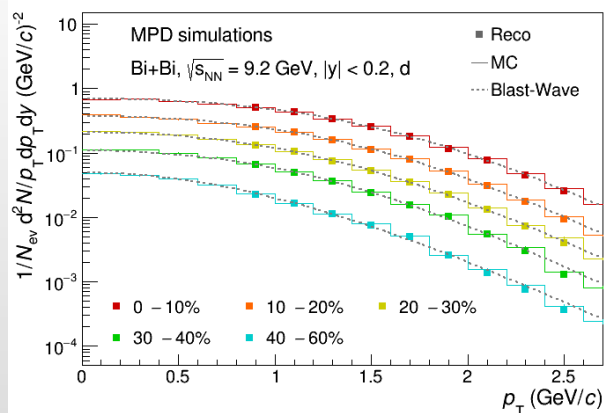




- ❖ MPD has excellent light fragment identification capabilities in a wide rapidity range

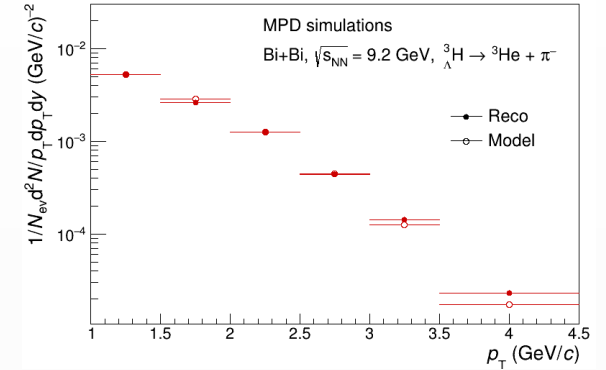
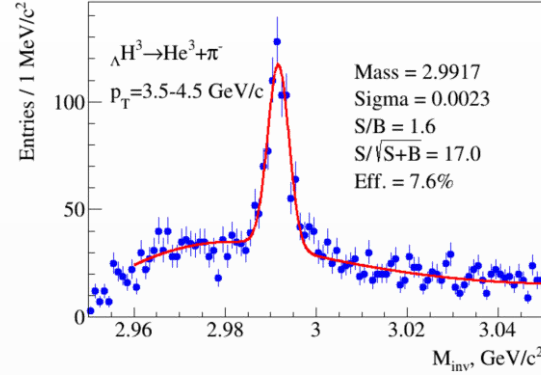
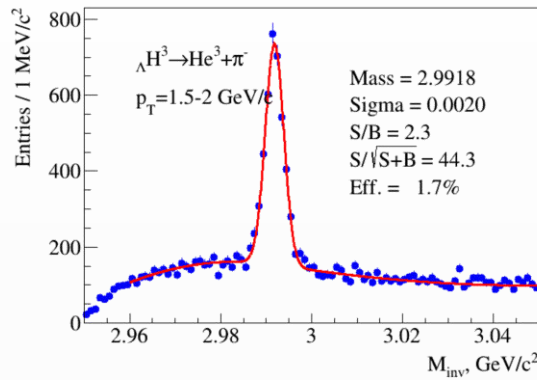


- ❖ Light nuclei reconstruction, Bi + Bi @ 9.2 GeV (PHQMD)



- ❖ NICA accelerator can deliver different ion beam species and energies → input to the heavy-ion data base for applied and space research to simulate damage from cosmic rays to astronauts, electronics, and spacecraft

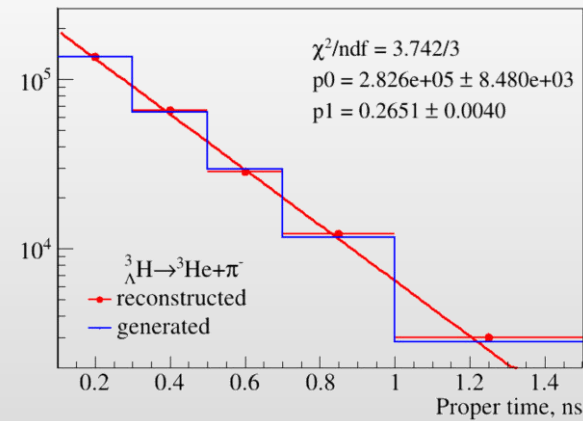
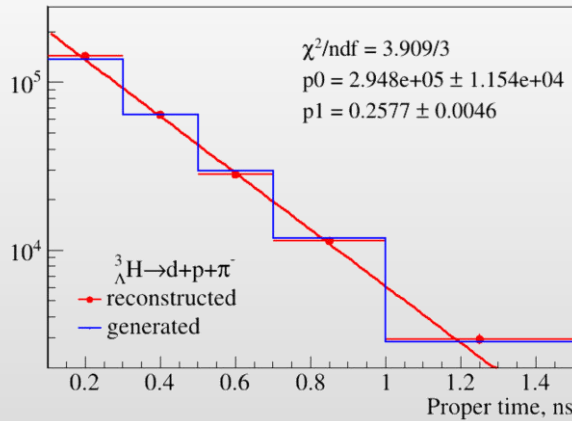
## ❖ Mass production 29 (PHQMD, BiBi@9.2 GeV, 40M events)



2- and 3-prong decay modes were studied separately to estimate systematics

$$N(\tau) = N(0) \exp\left(-\frac{\tau}{\tau_0}\right) = N(0) \exp\left(-\frac{ML}{cp\tau_0}\right),$$

Decay channel	Branching ratio	Decay channel	Branching ratio
$\pi^- + {}^3He$	24.7%	$\pi^- + p + p + n$	1.5%
$\pi^0 + {}^3H$	12.4%	$\pi^0 + n + n + p$	0.8%
$\pi^- + p + d$	36.7%	$d + n$	0.2%
$\pi^0 + n + d$	18.4%	$p + n + n$	1.5%



$\Lambda H^3$  reconstruction with ~ 50M samples events

$\Lambda H^4, \Lambda He^4$  reconstruction with ~ 150M samples events

# Multi-Purpose Detector (MPD) Collaboration



*MPD International Collaboration was established in 2018  
to construct, commission and operate the detector*

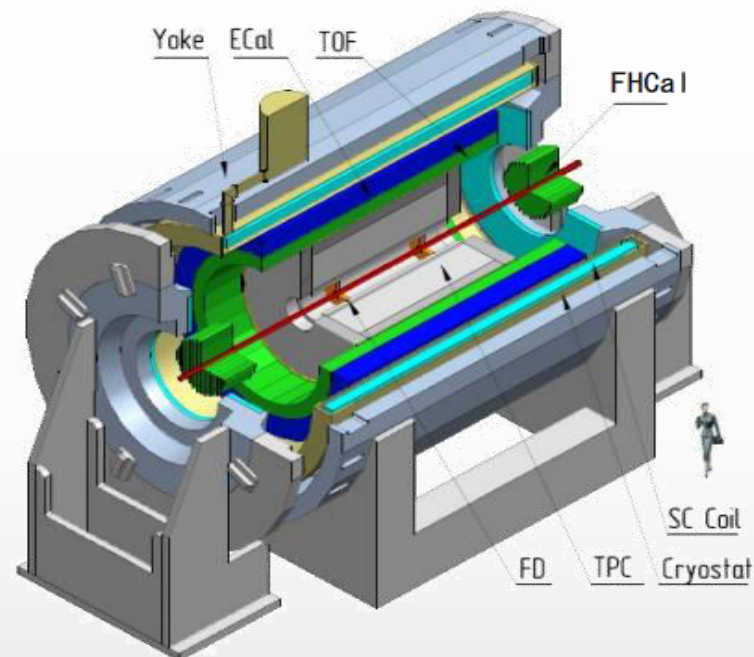
**12 Countries, >500 participants, 38 Institutions and JINR**

## Organization

**Acting Spokesperson:** **Victor Riabov**  
**Deputy Spokespersons:** **Zebo Tang, Arkadiy Taranenko**  
**Institutional Board Chair:** **Alejandro Ayala**  
**Project Manager:** **Slava Golovatyuk**

### **Joint Institute for Nuclear Research;**

A.Alikhanyan National Lab of Armenia, Yerevan, **Armenia**;  
Institute for Nuclear Problems of Belarusian State University, **Belarus**;  
Institute of Power Engineering of the National Academy of Sciences of Belarus, **Belarus**;  
SSI "Joint Institute for Energy and Nuclear Research - Sosny" of the National Academy of Sciences of Belarus, Minsk, **Belarus**;  
University of Plovdiv, **Bulgaria**;  
Tsinghua University, Beijing, **China**;  
University of Science and Technology of China, Hefei, **China**;  
Huzhou University, Huizhou, **China**;  
Institute of Nuclear and Applied Physics, CAS, Shanghai, **China**;  
Central China Normal University, **China**;  
Shandong University, Shandong, **China**;  
University of Chinese Academy of Sciences, Beijing, **China**;  
University of South China, **China**;  
Three Gorges University, **China**;  
Institute of Modern Physics of CAS, Lanzhou, **China**;  
Egyptian Center for Theoretical Physics, **Egypt**;  
Tbilisi State University, Tbilisi, **Georgia**;  
Institute of Physics and Technology, Almaty, **Kazakhstan**;  
Instituto de Ciencias Nucleares, UNAM, **Mexico**;  
Universidad Autónoma de Sinaloa, **Mexico**;  
Universidad Autónoma Metropolitana, **Mexico**;  
Universidad de Colima, **Mexico**;  
Universidad Michoacana de San Nicolás de Hidalgo, **Mexico**;  
Institute of Physics and Technology, **Mongolia**;



Belgorod National Research University, **Russia**;  
High School of Economics University, Moscow, **Russia**;  
Institute for Nuclear Research of the RAS, Moscow, **Russia**;  
National Research Nuclear University MEPhI, Moscow, **Russia**;  
Moscow Institute of Science and Technology, **Russia**;  
North Ossetian State University, **Russia**;  
National Research Center "Kurchatov Institute", **Russia**;  
National Research Tomsk Polytechnic University, **Russia**;  
Peter the Great St. Petersburg Polytechnic University Saint Petersburg, **Russia**;  
Plekhanov Russian University of Economics, Moscow, **Russia**;  
St.Petersburg State University, **Russia**;  
Skobeltsyn Institute of Nuclear Physics, Moscow, **Russia**;  
Petersburg Nuclear Physics Institute, Gatchina, **Russia**;  
Vinča Institute of Nuclear Sciences, **Serbia**;  
Pavol Jozef Šafárik University, Košice, **Slovakia**



## ❖ Shared Scientific Vision:

- ✓ India has strong heritage in nuclear and high-energy physics
- ✓ expertise in detector development, data analysis, and theoretical QCD
- ✓ active members of ALICE/STAR/CBM with important contributions

## ❖ MPD offers a unique energy range to explore dense baryonic matter

## ❖ Strategic Benefits for India:

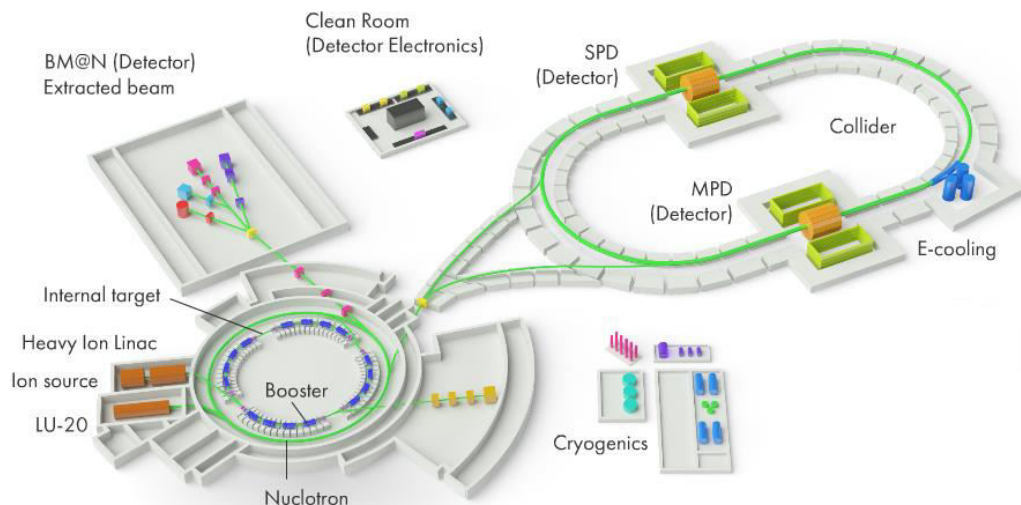
- ✓ training of young scientists and PhD students
- ✓ access to detector R&D
- ✓ open opportunities for Indian scientists in data analysis, software, and computing.



- ❖ Heavy-ion program at NICA → study of the QCD phase diagram in the region of maximum net-baryon density
- ❖ A comprehensive physics program to be studied for different ions (from p to Au) and collision energies ( $\sqrt{s_{NN}}$  from 2.4 to 11 GeV):
- ❖ NICA approaches its full commissioning → flagship project in the world on the study of heavy-ion collisions at intermediate energies
- ❖ MPD welcomes new members in the collaboration to participate in the comprehensive research programs

For more information please refer to <http://mpd.jinr.ru>

# BACKUP



- ❖ Heavy-ion beams, fixed-target and collider (up to Au,  $\mathcal{L} = 10^{27} \text{ cm}^{-2}\text{s}^{-1}$ ,  $\sqrt{s_{NN}} = 2.4\text{-}11 \text{ GeV}$ )  $\rightarrow$  strongly-interacting matter at extreme conditions of maximum baryonic density

Ion source (KRION-6T)  
Heavy Ion Linac (HILac)  
Booster

BM@N (Detector)  
MPD (Detector)

- ❖ Polarized beams of protons and deuterons in the collider (up to  $\mathcal{L} = 10^{32} \text{ cm}^{-2}\text{s}^{-1}$ ,  $\sqrt{s_{NN}} = 12.6 \text{ (d) } 27 \text{ (p) GeV}$ )  $\rightarrow$  nucleon spin structure research and clarification of the spin origin

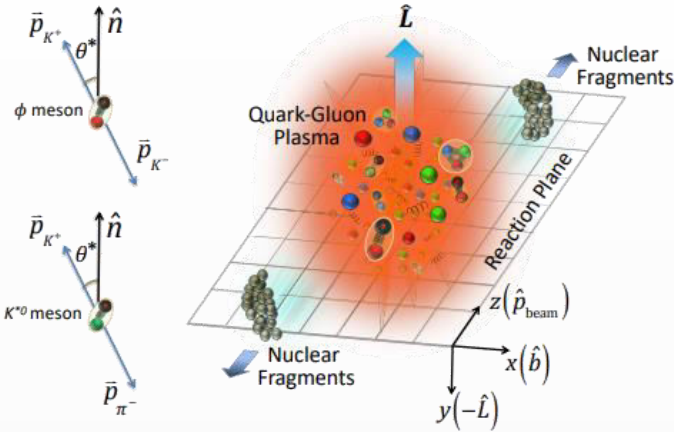
LU-20  
Nuclotron

SPD (Detector)

- ❖ Applied Research Infrastructure for Advanced Developments at NICA fAcility (ARIADNA)  $\rightarrow$  beam channels and irradiation stations for applied research with heavy-ion beams

- ❖ NICA project is approaching its full commissioning:
  - ✓ already running in fixed-target mode – BM@N, ARIADNA
  - ✓ start of operation in collider mode in 2026 – MPD and later SPD

Non-central heavy-ion collisions:



- ❖ If vector mesons are produced via recombination their spin may align
- ❖ Measured as anisotropies:

$$\frac{dN}{d\cos\theta} = N_0 [1 - \rho_{0,0} + \cos^2\theta (3\rho_{0,0} - 1)]$$

$\rho_{0,0}$  is a probability for vector meson to be in spin state = 0  $\rightarrow \rho_{0,0} = 1/3$  corresponds to no spin alignment

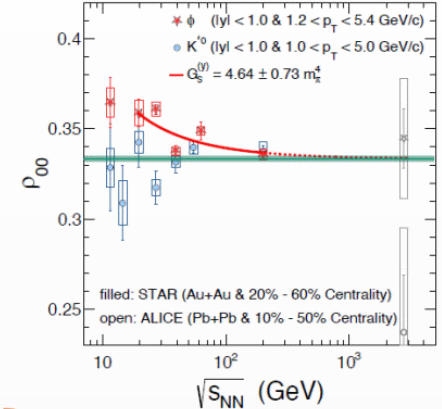
- ❖ Measurements at RHIC/LHC challenge theoretical understanding  $\rightarrow \rho_{00}$  can depend on multiple physics mechanisms (vorticity, magnetic field, hadronization scenarios, lifetimes and masses of the particles ...)

**MPD: extend measurements in the NICA energy range,  $\sqrt{s_{NN}} < 11$  GeV**

**The large  $\rho_{00}$  puzzle**

$$\rho_{00} \approx \frac{1}{3} + C_A + C_E + C_F + C_L + C_A + C_\phi + C_g$$

Physics Mechanisms	$\langle \rho_{00} \rangle$
$c_A$ : Quark coalescence vorticity & magnetic field <sup>[1]</sup>	$< 1/3$ (Negative $\sim 10^{-5}$ )
$c_E$ : E-comp. of Vorticity tensor <sup>[1]</sup>	$< 1/3$ (Negative $\sim 10^{-4}$ )
$c_E$ : Electric field <sup>[2]</sup>	$> 1/3$ (Positive $\sim 10^{-5}$ )
$c_F$ : Fragmentation <sup>[3]</sup>	$> \text{or}, < 1/3$ ( $\sim 10^{-5}$ )
$c_L$ : Local spin alignments <sup>[4]</sup>	$< 1/3$
$c_A$ : Turbulent color field <sup>[5]</sup>	$< 1/3$
$c_\phi$ : Vector meson strong force field <sup>[6]</sup>	$> 1/3$ (Can accommodate large positive signal)
$c_g$ : Glasma fields + effective potential	could be significant



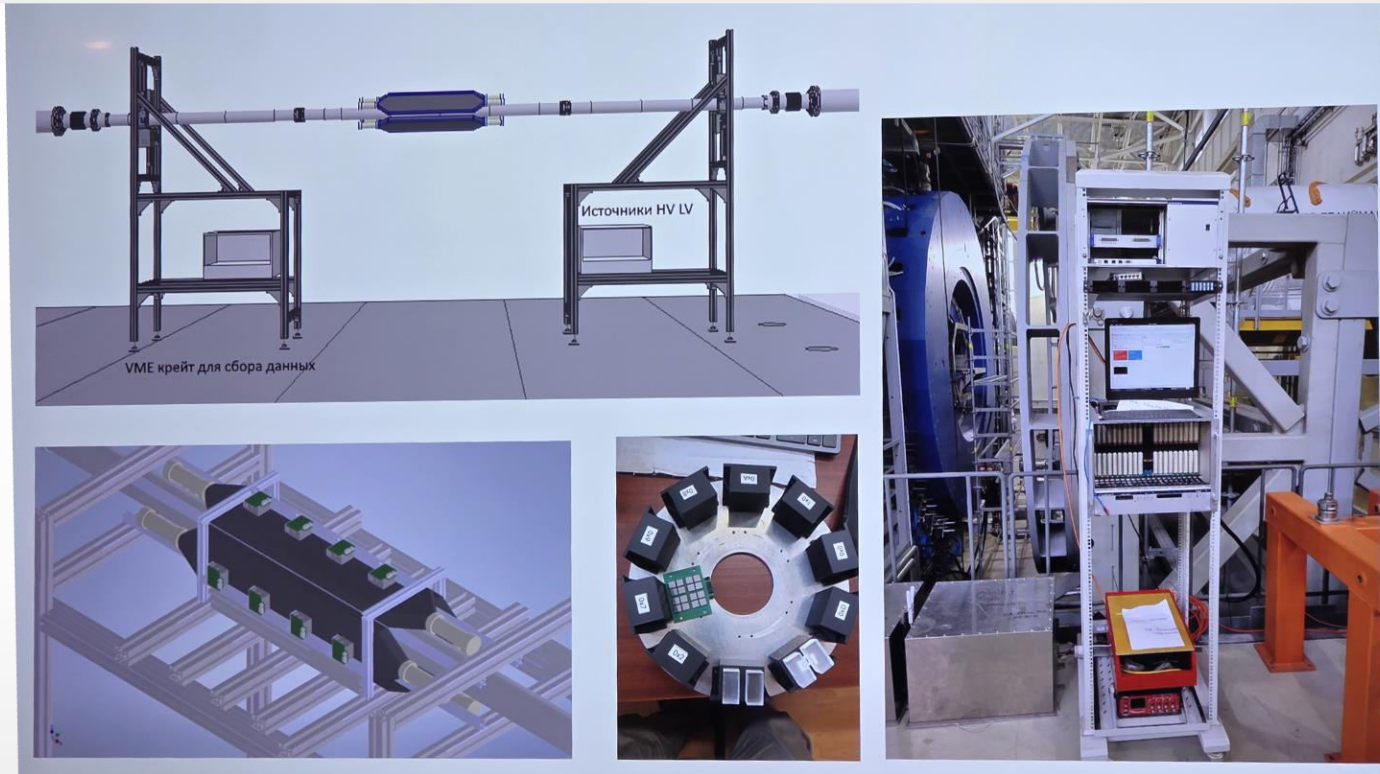
STAR, Nature 614 244 (2023)  
 Nature 614 244 (2023)

$\phi$  exhibits surprisingly large global spin alignment while  $K^*$  displays little.

Aihong Tang, QuarkMatter 2023, Houston, Sept 3-9

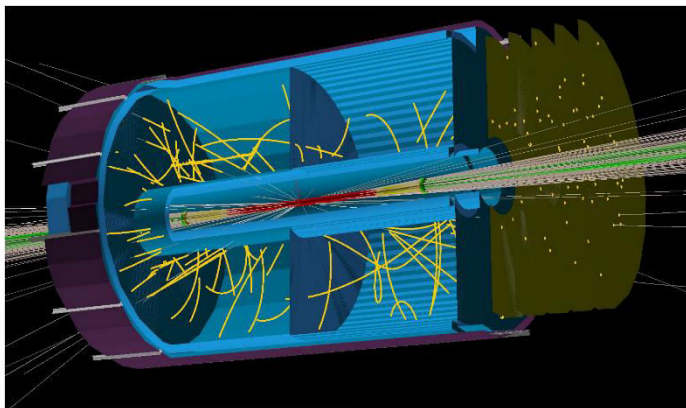


# Collider start-up configuration



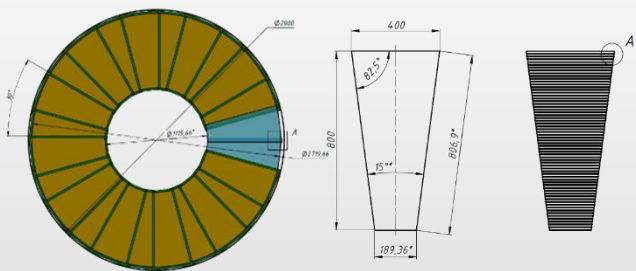
- ❖ FXT:
  - ✓ high event rate, high multiplicity → luminosity detector efficiently registers inelastic A-A collisions
- ❖ CLD:
  - ✓ low luminosity → low event rate for inelastic collisions ( $\sim 1 \text{ Hz at } 10^{24} \text{ cm}^{-2}\text{s}^{-1}$ )
  - ✓ use electromagnetic radiation from ultra peripheral collisions  
(huge cross section  $\sim 8,000 \text{ b}$ , but small multiplicity and soft electrons) → detect soft  $e^+/e^-$  and photons (511 KeV) from positron annihilation ( $\sim 1 \text{ Hz at } 10^{22}\text{-}10^{23} \text{ cm}^{-2}\text{s}^{-1}$ )

## Conception of the Forward Tracker (FTD)



- ✓ five tracking layers within  $z = 210\text{--}300$  cm,
- ✓  $1\% X_0 \sim 80 \mu\text{m}$  spatial resolution

## Conception of the end-cup TOF detector

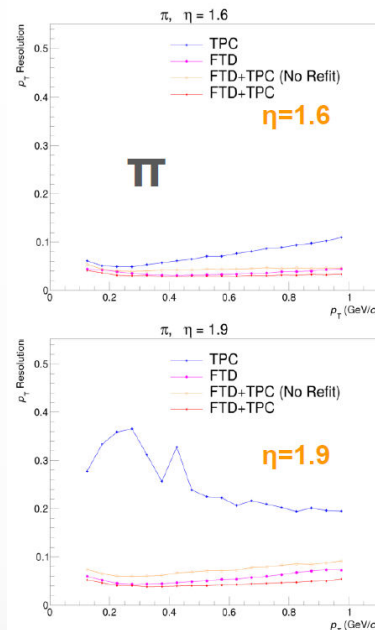


- ✓ each MRPC chamber contains 64 strips, which both-sides read-out
- ✓ each TOF ring contains 24 MRPCs  $\rightarrow$  6144 read-out channels in total
- ✓ same electronics based on NINO and HPTDC chips as in the basic TOF-MPD

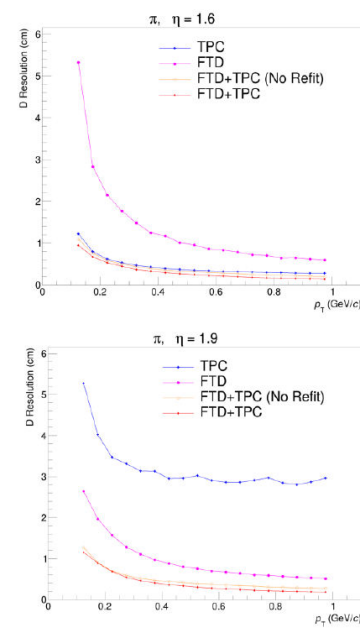
## Realistic event generators (UrQMD) + ACTS tracking

(FTD+TPC) makes possible track reconstruction up to  $\eta \sim 2$  with momentum resolution  $< 10\%$

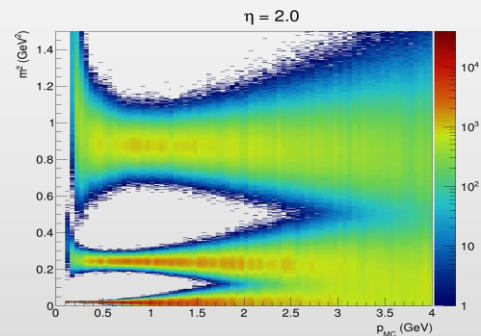
### Momentum resolution



### DCA resolution



### $\pi/K/p$ separation vs. particle momentum



# Direct photons and system temperature

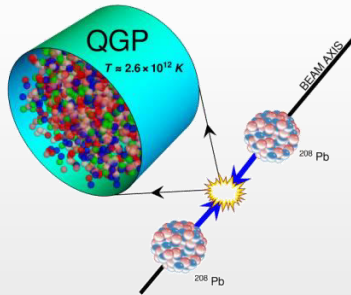
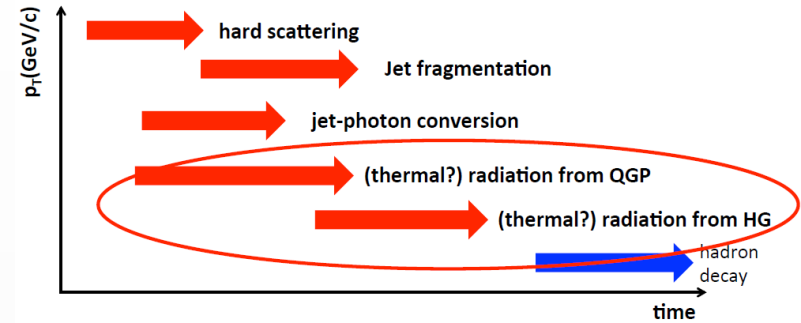
- All photons not from the hadron decays:
  - ✓ produced during all stages of the collision → penetrating probe
- Thermal low-E photons → effective temperature of the system:

$$E_\gamma \frac{d^3 N_\gamma}{d^3 p_\gamma} \propto e^{-E_\gamma / T_{\text{eff}}}$$

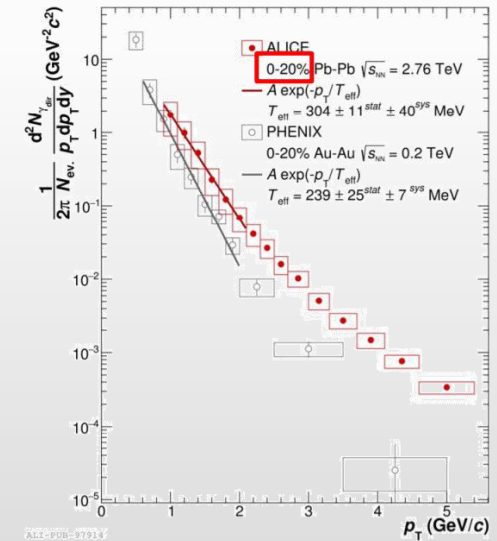
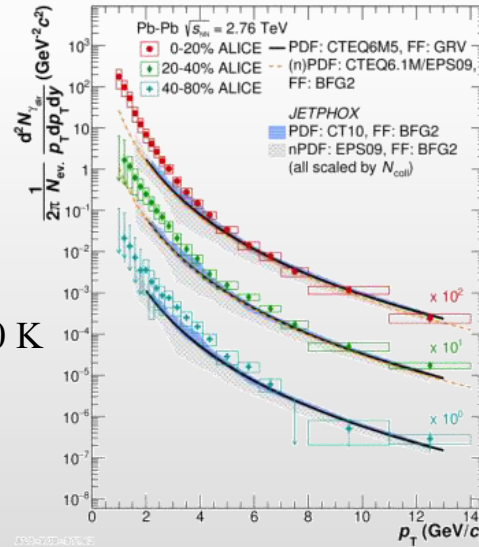
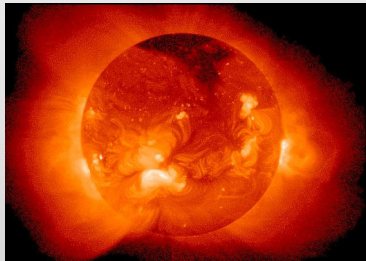
- Prompt higher- $p_T$  photons:

$$E \frac{d^3 \sigma}{dp^3} = \sum_{i,j,k} f_i(x_i, Q^2) \otimes f_j(x_j, Q^2) \otimes D_k(z_k, Q^2) \propto 1/p_T^n$$

- Relativistic A+A collisions → the highest temperature created in laboratory  $\sim 10^{12}$  K



Temperature at the center of the Sun  $\sim 15\,000\,000$  K



$T_{\text{eff}} \sim 240$  MeV at RHIC;  $T_{\text{eff}} \sim 300$  MeV at the LHC  
 $T_{\text{eff}} \gg T_c \sim 160$  MeV predicted by LQCD

A medium of  $\sim 200$  MeV is **100 000 times hotter !!!**

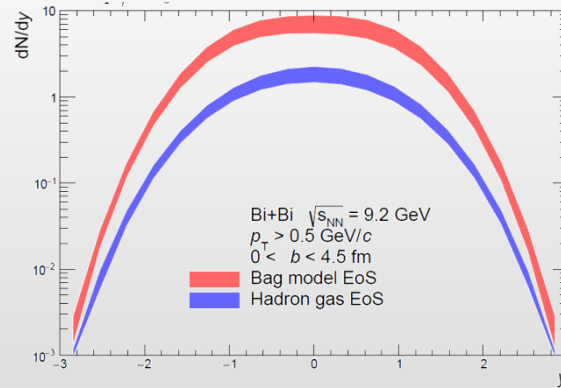
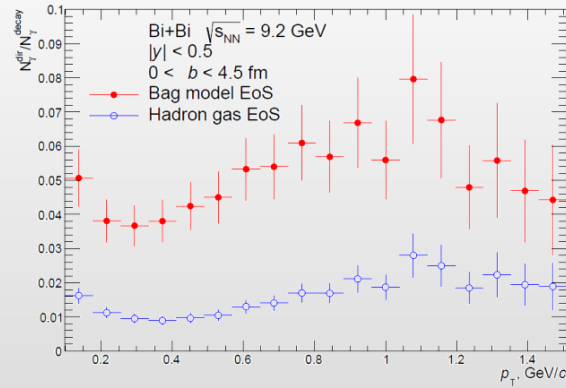
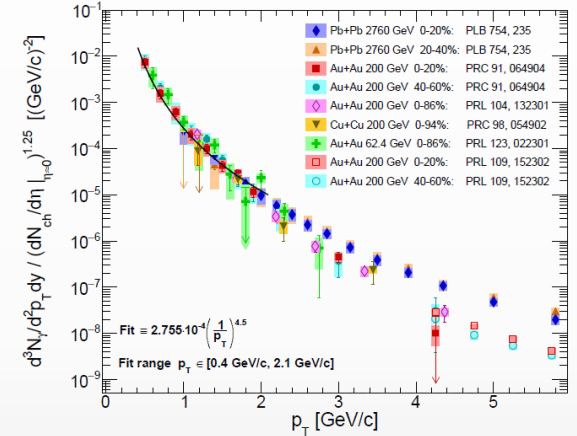
# Direct photon yields at NICA

Estimation of the direct photon yields @NICA

model  
calculations

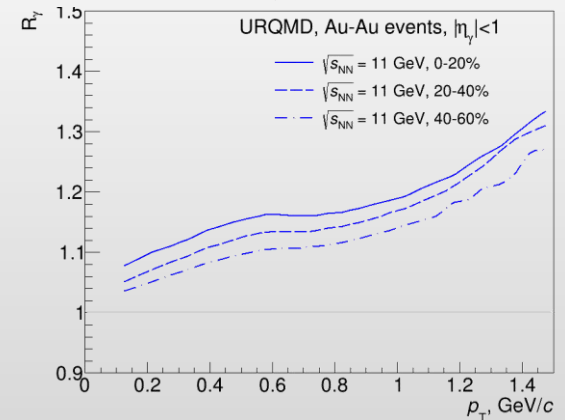
empirical  
scaling by PHENIX

- ✓ UrQMD v3.4 with hybrid model (3+1D hydro, bag model EoS, hadronic rescattering and resonances within UrQMD)
- ✓ each cell have  $T_i, E_i, \mu_{B,i}$ :
  - $T$  is high – QGP phase (Peter Arnold, Guy D. Moore, Laurence G. Yaffe, JHEP 0112:009 2001)
  - $T$  is low – HG phase (Simon Turbide, Ralf Rapp, Charles Gale, Phys.Rev.C69:014903,2004)
  - $T$  is intermediate – mixed phase
- ✓ integrate over all cells and all time steps
- ✓ calculations reproduce hydro calculations for the SPS



$$R_\gamma = \frac{\gamma_{inc}}{\gamma_{decay}} = \frac{\gamma_{inc}/\pi^0}{\gamma_{decay}/\pi^0_{param}}$$

$$\gamma_{direct} = \left(1 - \frac{1}{R_\gamma}\right) \cdot \gamma_{inc}$$



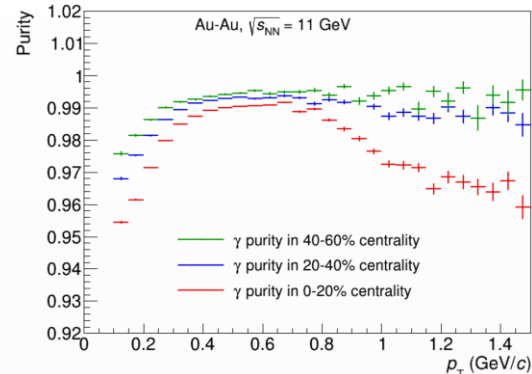
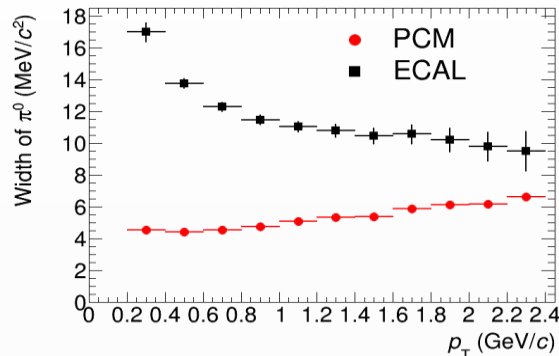
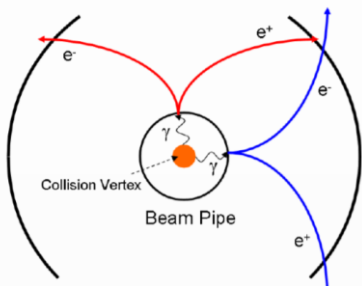
❖ Non-zero direct photon yields are predicted with  $R_\gamma \sim 1.05 - 1.15$  and  $v_2 \sim 0.5\%$  at top NICA energy



# Prospects for the MPD

- ❖ Photons can be measured in the ECAL or in the tracking system as  $e^+e^-$  conversion pairs (PCM)

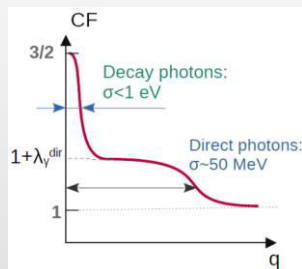
beam pipe (0.3%  $X_0$ ) + inner TPC vessels (2.4%  $X_0$ )



- ❖ Main sources of systematic uncertainties for direct photons → **potential yield measurements:**

- ✓ detector material budget → conversion probability;  $p_T$ -shapes and reconstruction efficiencies of  $\pi^0$  and  $\eta$
- ✓ with  $R_\gamma \sim 1.1$  and  $\delta R_\gamma/R_\gamma \sim 3\%$  → uncertainty of  $T_{\text{eff}} \sim 10\%$

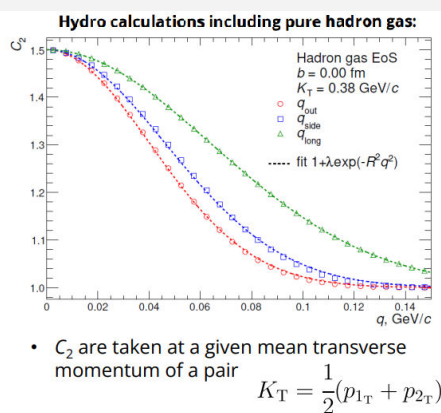
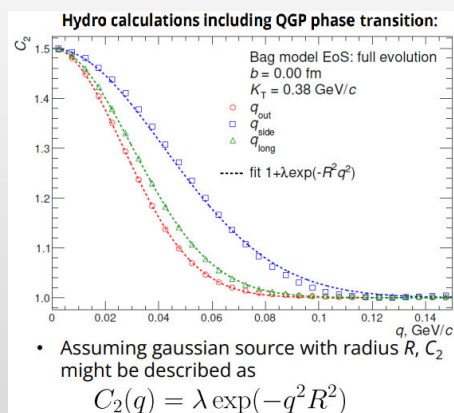
- ❖ **Measurement of Bose-Einstein correlations** for direct photons:



$$C_2(q, K) \approx 1 + \frac{\left| \int d^4x S(x, K) e^{iq \cdot x} \right|^2}{\left| \int d^4x S(x, K) \right|^2}$$

**Kinematics variables:**

- Relative momentum of the pair:  $q = p_1 - p_2$
- Mean pair momentum:  $K = \frac{1}{2}(p_1 + p_2)$



- ✓ Correlation function are different for QGP and HG scenario, the presence of the mixed phase causes increasing of the lifetime
- ✓ Possibility to extract yields of direct photons at low  $p_T$ :

$$\lambda = \frac{1}{2} \left( \frac{N_\gamma^{\text{dir}}}{N_\gamma^{\text{inc}}} \right)^2 \rightarrow R_\gamma = \frac{N_\gamma^{\text{inc}}}{N_\gamma^{\text{decay}}} = \frac{1}{1 - \sqrt{2}\lambda}$$

**MPD can potentially provide measurements for direct photon production in the NICA energy range**